Green nested simulation via likelihood ratio: Applications to longevity risk management

Ben Mingbin Feng [a],*, Johnny Siu-Hang Li [a], Kenneth Q. Zhou [b]

[a] *University of Waterloo, Canada*
[b] *Arizona State University, United States*

ABSTRACT

In the context of longevity risk, the nested simulation problem arises in various applications such as evaluating the effectiveness of longevity hedges and estimating solvency capital requirements. The standard nested simulation method demands a lot of computational effort, thereby making risk analyses in these applications difficult, especially in a practical setting when computing power is constrained. In this paper, we propose a green nested simulation (GNS) procedure for longevity risk management. The GNS procedure requires only small computations, achieves high accuracies, and is easy to implement. Mathematically, the GNS estimator is unbiased, and, in different modes of convergence, can achieve an arbitrary accuracy as the simulation budget increases. We demonstrate the GNS procedure with three numerical case studies. The empirical results indicate that the GNS procedure leads to estimates that are orders of magnitudes more accurate compared to the standard nested simulation, and also outperforms the existing approximation methods for getting around the nested simulation problem, particularly when the payoff under consideration is non-linear.

1. Introduction

1.1. Background

Simulation is a common analytical tool in longevity risk analyses, as prevalent stochastic mortality models including those considered by Cairns et al. (2009), Dowd et al. (2010) and Li et al. (2020) do not come with closed form expressions for moments or other risk measures of actuarial quantities. There are a number of exceptions such as the models of Lin and Liu (2007) and Kim et al. (2017), but the scope of the available closed form solutions is rather limited. Simulation of future mortality scenarios is therefore an important topic in the field of longevity risk.

Notable contributions on this topic include the multivariate normal method considered by Brouhns et al. (2002b), the parametric bootstrapping method proposed by Brouhns et al. (2005), the residual bootstrapping method introduced by Koissi et al. (2006), a modified semi-parametric bootstrapping method contributed by Yang et al. (2015), a Bayesian method considered by Czado et al. (2005), and a non-parametric method implemented by Li and Ng (2011). We refer readers to Renshaw and Haberman (2008) and Li (2014) for detailed reviews of these simulation methods. In the aforementioned works, the set-up is constructed to allow the user to simulate 'spot' mortality scenarios, which involve sample paths of mortality rates from now (i.e., the forecast origin $t = 0$) to a certain future time point. By evaluating an actuarial quantity (e.g., the present value of a life annuity) for each simulated sample path, an empirical probability distribution of the actuarial quantity, given information up to and including time $t = 0$, can be obtained. In the context of longevity risk management, spot mortality scenarios facilitate the analysis of cash flow hedges, which hedge against the exposure to variability in the future cash flows of mortality-related liabilities.

---

* Corresponding author.
  E-mail address: ben.feng@uwaterloo.ca (B.M. Feng).

Other than spot mortality scenarios, 'forward' mortality scenarios are needed in some contexts where the quantity of interest is the value of a mortality-related security, liability or portfolio at a certain future time point, say τ, where $\tau > 0$. To explain such contexts in more detail, let us suppose that the quantity of interest is

$$V_\tau = \mathbb{E}[H|\mathcal{F}_\tau], \tag{1}$$

where H represents the sum of the discounted cash flows arising from a mortality-related security, liability or portfolio, and $\mathcal{F}_t$ denotes the information up to and including time t. The cash flows associated with H depend on the evolution of mortality rates up to time T, where $T > \tau$. We can interpret V_τ as the time-τ value of the mortality-related security, liability or portfolio, and obviously, V_τ is a random variable when measured now (at time $t = 0$). In this setting, risk analysis amounts to estimating the (empirical) distribution of V_τ given $\mathcal{F}_0$, from which risk measures $\rho(V_\tau)$ such as Value-at-Risk (VaR) may be derived. One example of the setting underpinned by equation (1) is the evaluation of a value hedge, which hedges against the exposure to changes in the fair value of a mortality-related liability. In this situation, we first treat V_τ as the time-τ value of the naked position of the hedger's mortality-related liability, and then treat V_τ as the time-τ value of the hedged position which includes some mortality-related hedging instruments. The effectiveness of the value hedge can be calculated by comparing the risk measures derived from the two empirical distributions involved. Another example is the calculation of Solvency Capital Requirements (SCR) under Solvency II. In this context, we specifically calculate the Value-at-Risk from the distribution of V_1, the value of the insurer's mortality-related liability one year from now.

The setting underpinned by equation (1) represents a nested simulation problem (Hong et al., 2017). To estimate the distribution of V_τ given $\mathcal{F}_0$ and its associated risk measures $\rho(V_\tau)$ using the standard nested simulation, one first simulates M independent realizations of mortality rates up to and including time τ; then, conditioning on each outer scenario, one simulates N independent 'forward' mortality scenarios involving mortality rates from time $\tau + 1$ to T, which allow us to calculate a realization of $V_\tau = \mathbb{E}[H|\mathcal{F}_\tau]$ as the sample average of the N realizations of H implied by the forward mortality scenarios in the inner loop. The M realizations of V_τ form an empirical distribution of V_τ, from which risk measures $\rho(V_\tau)$ can be estimated. In the standard nested simulation, a simulation budget of $\Gamma = MN$ inner simulations is required. Depending on the complexities of H and the assumed stochastic mortality model, the simulation budget Γ may be prohibitively excessive.

Despite being practically relevant, the computational work entailed in the set-up underpinned by equation (1) has not been studied as much as one would expect. In the actuarial literature, Cairns (2011) and Dowd et al. (2011) proposed a method that spares the user from the need of implementing the inner loop through a Taylor's approximation of the survival functions involved in H. However, as we demonstrate in our case studies, this method has some limitations and does not always produce satisfactory results. By drawing on recent developments in the operations research domain, in this paper we contribute an efficient nested simulation procedure that is applicable to longevity risk analyses in which forward mortality scenarios are needed.

1.2. Relevant studies in the operations research domain

Before we detail our contribution, let us review some key operations research literature that is closely related to our research problem. Concerning the alleviation of the computational burden in nested simulations, one research venue aims to optimally allocate a fixed simulation budget between the inner- and outer-simulations that achieves fast convergence. Under some assumptions, Gordy and Juneja (2010) show that the optimal asymptotic mean squared error (MSE) of the standard nested risk estimator converges at $\mathcal{O}(\Gamma^{-2/3})$ when $M = \mathcal{O}(\Gamma^{-2/3})$ and $N = \mathcal{O}(\Gamma^{-1/3})$. Broadie et al. (2011) considers sequential simulation procedures whose MSE converges at $\mathcal{O}(\Gamma^{-4/5+\varepsilon})$ for any $\varepsilon > 0$. Another line of research aims to identify efficient alternatives to replace inner simulations. The well-known least-squares Monte Carlo (LSMC) (Longstaff and Schwartz, 2001; Tsitsiklis and Van Roy, 2001) uses a parametric regression in place of inner simulations for pricing American option is one such example. Broadie et al. (2015) use LSMC in risk management problems and show that the MSE of the resulting risk estimator converges at $\mathcal{O}(\Gamma^{-1})$ until reaching an asymptotic squared bias level. Practical applications of LSMC are precluded by its dependence on the choice of basis functions. Hong et al. (2017) propose a kernel smoothing approach that replaces inner simulations with the Nadaraya-Watson kernel estimator, whose MSE converges at $\mathcal{O}(\Gamma^{-\min\{1,4/(d+2)\}})$, where d is the dimension of the problem. The performance of the kernel smoothing approach depends on the bandwidth parameter in the Nadaraya-Watson estimator, which is often difficult and time-consuming to tune. Lan et al. (2010) use ranking-and-selection techniques to improve the efficiency of inner simulations. Liu et al. (2010) and Feng and Staum (2017) propose simulation procedures to replace inner simulations with stochastic kriging (Mehdad and Kleijnen, 2018), which is sometimes difficult to implement due to its numerical instability (Staum, 2009). To the best of our knowledge, no convergence property has been shown for nested simulation procedures based on stochastic kriging.

1.3. Our contribution

One contribution in this study is the development and analysis of an efficient simulation procedure for estimating $\rho(V_\tau)$ and its application in the risk measurement for longevity-linked securities. The proposed simulation procedure requires small computations, achieves high accuracies, and is easy to implement. One inspiration for our study is green simulation, which was first proposed by Feng and Staum (2016) and Feng and Staum (2017) to reuse simulation outputs in repeated experiments, such as periodic risk monitoring simulations with updated market information. Feng and Staum (2017) mainly study green simulation via likelihood ratio methods. Likelihood ratio estimators have also been used for pricing American options (Broadie et al., 2000; Broadie and Glasserman, 2004; Avramidis and Hyden, 1999; Avramidis and Matzinger, 2004), and are commonly known as stochastic mesh methods in that context. In this study, we use likelihood ratio estimators in nested simulation problems, with a goal to reuse the all of the inner simulation outputs to improve accuracies for all the outer scenarios. The nested estimation problems considered in this study are different from American option pricing, which is a stochastic control problem.

1.4. Organization

The remainder of this article is organized as follows. Section 2 presents the set-up and the nested risk estimation problem. It also summarizes the information that is necessary in the exposition of our proposed simulation procedure, including that concerning stochastic mortality models, mortality-linked securities, and valuation methods. Section 3 discusses the methodological development and theoretical analysis of the proposed simulation procedure. Section 4 features three case studies that concern three different mortality-linked securities, respectively. Finally, Section 5 concludes.

2. Settings and backgrounds

In this section, we first describe the set-up on which the proposed simulation method is developed, and state the simplifying assumptions we make. We then briefly review the Lee-Carter model which we use as an example model to explain the proposed simulation method. The review is followed by a description of the mortality-linked liabilities and securities, which we consider in our numerical case studies. Finally, a critical review of the existing methods for dealing with the problem in question is provided.

2.1. Set-up

We consider simulations from typical discrete-time stochastic mortality models, including but not limited to those mentioned in the works of Cairns et al. (2009) and Dowd et al. (2010). The models are built upon an age-period-cohort structure, which are estimated to historical death and exposure counts by means of a maximum likelihood or Bayesian method. A general formula for such a structure is provided by Villegas et al. (2018). The structure allows the modeler to extract certain signals that depend on either time (period effects) or year-of-birth (cohort effects), which may be considered as drivers of mortality dynamics. Such signals are then extrapolated through certain stochastic processes to obtain forecasts of future mortality. Our simulation work therefore surrounds the stochastic processes for period and cohort effects. Although period and cohort effects are typically represented by Greek letters kappa and gamma, respectively, in this paper we use κ_t to represent the vector of period effects at time t and cohort effects for year-of-birth $t - x$ (for a fixed age x).

Let $\{\kappa_t, t = 0, 1, \ldots\}$ be a discrete-time stochastic time series that encodes the time-t value of the underlying period and cohort effects, which determines the cash flows associated with some mortality-linked liabilities and securities of interest. To simplify the presentation of the proposed simulation method, we assume that $\{\kappa_t\}$ is a Markovian process with a natural filtration $\mathcal{F}_t$. It should be noted that this is not a required assumption, because a typical non-Markovian process can be turned into a Markovian process through an extension of the state space.

Consider a mortality-linked security or liability (see Section 2.3 for examples), whose value at time t depends on κ_t. Suppose that the current time is $t = 0$ and that the security/liability matures at some future time $T > 0$. For any $t = 1, 2, \ldots, T$, we denote the security's time-t value by $V_t = V(\kappa_t)$, which is the conditional expectation of the sum of all discounted cash flows associated with the security beyond time t given the value of κ_t. When viewed at the current time $t = 0$, V_t for $t > 0$ is a random variable whose randomness arises from the stochastic evolution of $\{\kappa_t\}$.

We let $\tau \in (0, T)$ be the prescribed *risk horizon*. For instance, when considering the 1-year Value-at-Risk for SCR calculations under Solvency II, τ is set to one (year). For notational convenience, we denote the values of period and/or cohort effects *beyond* τ by

$$\kappa_{\tau+} := \{\kappa_{\tau+1}, \ldots, \kappa_T\}.$$

We further assume that for any $0 \leq s < t \leq T$ the conditional probability density function of κ_t given κ_s, i.e., $f(\kappa_t|\kappa_s)$, is well-defined; with a slight abuse of notation we also write $f(\kappa_{\tau+}|\kappa_\tau) = f(\kappa_T|\kappa_{T-1})f(\kappa_{T-1}|\kappa_{T-2}) \cdots f(\kappa_{\tau+1}|\kappa_\tau)$. It follows that the time-τ value V_τ can be written as

$$V_\tau = V(\kappa_\tau) = \mathbb{E}[H(\kappa_{\tau+})|\mathcal{F}_\tau] = \mathbb{E}[H(\kappa_{\tau+})|\kappa_\tau] = \int H(\kappa_{\tau+})f(\kappa_{\tau+}|\kappa_\tau)d\kappa_{\tau+}, \tag{2}$$

where $H(\kappa_{\tau+})$ is the security's discounted future payoffs (discounted to time τ at a constant interest rate of r per period for any duration) given the realization of future risk factor $\kappa_{\tau+}$. Note that $\mathbb{E}[H(\kappa_{\tau+})|\mathcal{F}_\tau] = \mathbb{E}[H(\kappa_{\tau+})|\kappa_\tau]$ because κ_t is assumed Markov.

To further ease exposition, we assume in our presentation that the simulation model is the Lee-Carter model, which contains only one stochastic factor (a period effect) so that κ_t is a scalar. With some notational changes, the framework presented in the following sections can be extended easily to include a wide range of mortality models, including those that fit into the general specification defined by Villegas et al. (2018).

2.2. The Lee-Carter model

Let $m_{x,t}$ be the central death rate at age x and in year t. The Lee-Carter model (Lee and Carter, 1992) is specified as

$$\ln m_{x,t} = \alpha_x + \beta_x \kappa_t, \tag{3}$$

where

- α_x is an age-specific parameter capturing the average level of mortality at age x,
- κ_t is a time-varying index (i.e., the period effect) reflecting the overall level of mortality in year t, and
- β_x is an age-specific parameter measuring the sensitivity of $\ln m_{x,t}$ at age x to changes in κ_t.

Equation (3) does not contain an error term, because we assume a Poisson error structure in which the error for each age-time cell is represented by the difference between the actual death count and the death count implied by the model.

Following Lee and Carter (1992), the period effect is modeled by a random walk with drift, i.e.,

$$\kappa_t = \kappa_{t-1} + \theta + \epsilon_t, \quad \epsilon_t \sim \mathcal{N}(0, \sigma_\epsilon^2) \tag{4}$$

where the drift θ represents the per-period change in κ_t and σ_ϵ^2 is the constant variance for the independent noises ϵ_t, $t = 1, \ldots, T$. Given fixed values of θ and σ_ϵ^2, the period effect κ_t follows a random walk, which is a Markovian process. For any $0 \le s < t \le T$, the conditional distribution of κ_t given κ_s is given by

$$f(\kappa_t | \kappa_s) \sim \mathcal{N}(\kappa_s + (t-s)\theta, (t-s)\sigma_\epsilon^2), \tag{5}$$

where $\mathcal{N}(\mu, \sigma^2)$ denotes the normal distribution with a mean of μ and a variance of σ^2.

On the basis of the model specification, one can obtain expressions for demographic functions such as survival probabilities. Let $S_{x,t}(u)$ be the *ex post* probability that an individual aged x at time t would have survived to time $t + u$. Under the assumption that the force of mortality between two consecutive integer ages is constant, one can show that

$$S_{x,t}(u) = \prod_{s=1}^{u} e^{-m_{x+s-1,t+s}}, \quad t, u \ge 0, \tag{6}$$

where $m_{x+s-1,t+s}$ is the central death rate at age $x + s - 1$ and in year $t + s$ as specified in the Lee-Carter model. Putting equation (3) into (6), we get

$$S_{x,t}(u) = \exp\left(-\sum_{s=1}^{u} \exp(\alpha_{x+s-1} + \beta_{x+s-1}\kappa_{t+s})\right), \tag{7}$$

an expression that is used heavily when defining the value of a life annuity (Section 2.3.3).

Using equation (7), we can further obtain an expression for the (conditional) probability that an individual aged x at time $t - 1$ dies between time $t - 1$ and t:

$$q_{x,t} = 1 - S_{x,t-1}(1) = 1 - \exp\left(-\exp(\alpha_x + \beta_x \kappa_t)\right). \tag{8}$$

The payoff of some mortality-linked securities, such as q-forwards and q-spreads (Section 2.3.2), directly depend on the observed value of $q_{x,t}$ for a certain combination of x and t.

2.3. Mortality-linked securities and liabilities

In this section, we specify three mortality-linked securities/liabilities, namely, K-option, q-call-spread, and temporary life annuity, and relate them to the set-up presented in Section 2.1.

2.3.1. K-options

We first discuss K-options, a category of hypothetical mortality-linked securities that was first introduced by Li et al. (2021). Although K-options have not been traded in real-life, it is important to consider them in this study because under certain model assumptions they come with closed-form valuation formulas, which enable us to benchmark the accuracy of our proposed simulation method.

Let us consider a K-call option with strike value K and maturity T. It has a payoff of $(\kappa_T - K)^+ = \max\{\kappa_T - K, 0\}$ per \$1 notional at maturity. At time $\tau < T$, its discounted payoff is

$$H(\kappa_{\tau+}) = H(\kappa_T) = e^{-r(T-\tau)} \cdot (\kappa_T - K)^+, \tag{9}$$

where r is the applicable continuously compounded discount rate per annum. Its time-τ value is $V(\kappa_\tau) = \mathbb{E}[H(\kappa_T)|\kappa_\tau]$.

A K-put option with the same strike and maturity has a payoff of $(K - \kappa_T)^+$ per \$1 notional at maturity. Its time-τ discounted payoff and time-τ conditional expected value are specified similarly.

We observe from (9) that a K-option's discounted payoff depends only on the terminal value of the risk factor, i.e., κ_T, but not any of the intermediate values between τ and T. Such a payoff can therefore be regarded as *non-path-dependent*, just as the payoffs of typical European-style financial options. Non-path-dependent payoffs are usually simpler to evaluate compared to path-dependent ones, and may enable analytical valuation. For example, under the Lee-Carter model, a K-option's time-τ value $V(\kappa_\tau)$ can be calculated analytically.

2.3.2. Call spreads

Generally speaking, a call spread has a payoff of

$$\max\left(\min\left(\frac{x - AP}{EP - AP}, 1\right), 0\right)$$

per \$1 notional at maturity T, where x represents the value of the underlying at time T, and AP and EP ($AP < EP$) are the attachment point and exhaustion point, respectively.

Cairns and El Boukfaoui (2021) brought call spreads to the context of mortality-related risks. In this context, the underlying x can be, for example, the time-T value of the Lee-Carter mortality index (i.e., κ_T), and the value of $q_{x,T}$. The payoff structure enables the hedger to mitigate a specific portion (typically the more extreme portion) of mortality-related risks.

Note that a call spread's payoff can be decomposed into a long call with a strike of AP combined with a short call with a strike of EP, i.e.,

$$V(\kappa_\tau) = e^{-r(T-\tau)} \mathbb{E}\left[\max\left(\min\left(\frac{x - AP}{EP - AP}, 1 \right), 0 \right) \Big| \kappa_\tau \right]$$

$$= \frac{e^{-r(T-\tau)}}{EP - AP} \left(\mathbb{E}[(x - AP)^+|\kappa_\tau] - \mathbb{E}[(x - EP)^+|\kappa_\tau] \right).$$

Consequently, a call spread's time-τ value can be calculated analytically if one can calculate the call options' time-τ values analytically (e.g., K-options).

For illustration purposes, in this study we consider a q-call-spread with $x = q_{x,T} = 1 - S_{x,T-1}(1)$. The discounted payoff at time τ for a q-call-spread is given by

$$H(\kappa_{\tau+}) = H(\kappa_T) = e^{-r(T-\tau)} \max\left(\min\left(\frac{q_{x,T} - AP}{EP - AP}, 1 \right), 0 \right), \tag{10}$$

as so its time-τ value is $V(\kappa_\tau) = \mathbb{E}[H(\kappa_T)|\kappa_\tau]$. Although the q-call-spread has a non-path-dependent payoff, its time-τ value $V(\kappa_\tau)$ cannot be analytically calculated even under the Lee-Carter model, so simulation is needed.

2.3.3. Annuity liabilities

We consider a T-year temporary life annuity-immediate, payable to an individual who is aged x_0 at time 0. The annuity pays \$1 at the end of each year for T years as long as the annuitant is alive. The time-0 value of the annuity is $\sum_{u=1}^{T} e^{-ru} S_{x_0,0}(u)$, where $S_{x,t}(u)$ is the probability that an individual aged x at time t would survive to time $t + u$, as defined in Section 2.2. At time τ, a surviving policyholder will be at age $x + \tau$ and will be holding a $(T - \tau)$-year temporary life annuity-immediate. So the discounted payoff at time-τ is

$$H(\kappa_{\tau+}) = \sum_{u=1}^{T-\tau} e^{-ru} S_{x_0+\tau,\tau}(u). \tag{11}$$

The corresponding time-τ conditional expected value is then

$$V(\kappa_\tau) = \mathbb{E}[H(\kappa_{\tau+})|\kappa_\tau] = \sum_{u=1}^{T-\tau} e^{-ru} \mathbb{E}[S_{x_0+\tau,\tau}(u)|\kappa_\tau]. \tag{12}$$

Unlike K-options and q-call-spreads, a life annuity has a *path-dependent* payoff, because the payoff depends not only on the terminal value κ_T but also all the intermediate values, i.e., κ_t for all $t \in [\tau + 1, T]$. Such path dependency aggravates the computational burden in simulation.

2.4. Existing valuation methods

In the literature, there exist different methods to compute the time-τ value $V(\kappa_\tau)$ for different mortality-linked securities. We now review three existing valuation methods, which are then compared with our proposal.

2.4.1. Closed-form formulas

Analytical calculation of $V(\kappa_\tau)$ is accurate and requires minimal computational effort, but is only possible for certain simple securities and model assumptions. For instance, Lemma 2.1 summarizes the closed-form formulas of $V(\kappa_\tau)$ for K-options under the Lee-Carter model (3)–(4).

Lemma 2.1 (*Paraphrase of equation (7) in Li et al. (2021)*). *Suppose that the Lee-Carter model specified in equations* (3)–(4) *holds. The time-τ conditional expected value of a K-option is given by*

$$V(\kappa_\tau) = e^{-r(T-\tau)} \left[\sigma_k \cdot \phi\left(\frac{K - \mu_k}{\sigma_k} \right) + \lambda \cdot (K - \mu_k) \cdot \Phi\left(\frac{\lambda \cdot (K - \mu_k)}{\sigma_k} \right) \right], \tag{13}$$

where ϕ and Φ are the standard normal density and distribution functions, respectively, $\mu_k = \kappa_\tau + (T - \tau)\theta$, $\sigma_k = \sqrt{T - \tau} \cdot \sigma_\epsilon$, and $\lambda = 1$ (or $\lambda = -1$) for a put (or call, resp.) option.

Other securities such as q-call-spreads and temporary life annuities do not have analytical expressions for $V(\kappa_\tau)$ even under a simple model like the Lee-Carter model. Also, if the risk factor κ_t were to follow a complicated stochastic process, such as a stochastic process with jumps (Chen, 2013; Chen and Cox, 2009; Liu and Li, 2015; Zhou et al., 2013), then even simple securities such as K-options may not have a closed-form formula for $V(\kappa_\tau)$. In these cases, other valuation methods such as nested simulation may be needed to estimate $V(\kappa_\tau)$.

2.4.2. Standard nested simulation

The standard nested simulation is a common approach to obtain a random sample of $V(\kappa_\tau)$. The key steps include the following.

1. **Outer simulation**: Based on a given stochastic mortality model (e.g., the Lee-Carter model), simulate M independent outer scenarios $\kappa_\tau^{(i)}$, $i = 1, \ldots, M$.
2. Conditioning on each outer scenario, say $\kappa_\tau^{(i)}$, perform the following steps.

(a) **Inner simulation**: Simulate N independent sample paths of $\kappa_{\tau+}$ given $\kappa_\tau^{(i)}$ (i.e., $\kappa_{\tau+}^{(i,1)}, \ldots, \kappa_{\tau+}^{(i,N)}$) from the same density function $f(\kappa_{\tau+}|\kappa_\tau^{(i)})$. We refer $\{\kappa_{\tau+}^{(ij)}, j=1,\ldots,N\}$ to as the inner sample paths of the i-th scenario.

(b) Use the inner sample paths of i-th scenario to calculate the discounted payoffs $H(\kappa_{\tau+}^{(ij)})$, $j=1,\ldots,N$, and estimate the time-τ value $V(\kappa_\tau^{(i)})$ by

$$\widehat{V}_N^{ns}(\kappa_\tau^{(i)}) = \frac{1}{N} \sum_{j=1}^{N} H(\kappa_{\tau+}^{(ij)}). \tag{14}$$

3. Use the empirical distribution of the random sample $\{\widehat{V}_N^{ns}(\kappa_\tau^{(i)}), i=1,\ldots,M\}$ to estimate the risk measure $\rho(V_\tau)$ of interest.

The standard nested simulation is generally applicable to different mortality models and payoff structures, however complicated they might be. For any fixed scenario κ_τ, $\widehat{V}_N^{ns}(\kappa_\tau)$ is an unbiased estimator whose variance converges to zero, provided that it is finite, at a rate of $\mathcal{O}(N^{-1})$. Also, under some conditions one can show that the estimator for $\rho(V_\tau)$ converges to the true risk measure at a certain convergence rate (see, e.g., Gordy and Juneja, 2010).

Despite its flexibility and convergence properties, the standard nested simulation is notoriously known for its heavy computational burden, as it requires a simulation budget of $\Gamma = MN$ inner simulations. Depending on the complexity of the stochastic mortality model and the payoff structure, each inner simulation may be costly and the total simulation budget can be prohibitively excessive.

2.4.3. Approximation methods

Ignoring the outer scenarios' stochasticity, $V(\kappa_\tau)$ can be viewed as a real-valued function of κ_τ and thus can be approximated by, for example, a Taylor approximation. Provided that the required derivatives exist for some *anchor scenario* $\widetilde{\kappa}_\tau$, the Taylor approximation of $V(\kappa_\tau^{(i)})$ for the scenario $\kappa_\tau^{(i)}$ is given by

$$\widehat{V}^{app}(\kappa_\tau^{(i)}) \approx V(\widetilde{\kappa}_\tau) + \frac{V'(\widetilde{\kappa}_\tau)}{1!}(\kappa_\tau^{(i)} - \widetilde{\kappa}_\tau) + \frac{V''(\widetilde{\kappa}_\tau)}{2!}(\kappa_\tau^{(i)} - \widetilde{\kappa}_\tau)^2 + \cdots. \tag{15}$$

In particular, Lemma 2.2 presents the first-order Taylor approximation for a K-option under the Lee-Carter model. Note that, in this case, both the value function $V(\widetilde{\kappa}_\tau)$ and the derivative $V'(\widetilde{\kappa}_\tau)$ can be calculated analytically.

Lemma 2.2 (*Paraphrase of Section 5.2 in Li et al. (2021)*). *Suppose the Lee-Carter model specified in equations* (3)–(4) *hold. A first-order Taylor approximation for a K-option around some scenario $\widetilde{\kappa}_\tau$ is given by*

$$V(\kappa_\tau) \approx V(\widetilde{\kappa}_\tau) + e^{-r(T-\tau)} \cdot (\kappa_\tau - \widetilde{\kappa}_\tau) \cdot \Phi\left(\frac{\lambda \cdot (K - \widetilde{\kappa}_\tau - \theta(T-\tau))}{\sigma_\epsilon \sqrt{T-\tau}}\right) \tag{16}$$

where $V(\widetilde{\kappa}_\tau)$ is as defined in (13) *and $\lambda = 1$ (or $\lambda = -1$) for a put (or call, resp.) option.*

When analytical formulas for $V(\widetilde{\kappa}_\tau)$ and its required derivatives are not available, one can estimate them via simulation and then substitute the estimates into (15). In this study, we employ the so-called pathwise estimator, also known as the Infinitesimal Perturbation Analysis (IPA) (Glasserman, 2004), to estimate the required derivatives in (15). In Appendix A, we derive the estimators of $V'(\widehat{\kappa}_\tau)$ for q-call-spreads. For comparison purposes, we also derive in Appendix A the estimators of $V'(\widehat{\kappa}_\tau)$ for K-calls, even though analytical formulas are available. Furthermore, one can show that for option-like securities, such as K-options and q-spreads, the pathwise estimates for the second or higher order derivatives are zeros. Interested readers may refer to Chapter 7 in Glasserman (2004) and Chapter 5 in Fu et al. (2015) for other sensitivity/gradient estimation-via-simulation methods.

Besides the Taylor approximation (15), Cairns (2011) and Dowd et al. (2011) propose a probit-Taylor approximation for the expected survival probability $\mathbb{E}[S_{x,\tau}(u)|\kappa_\tau]$. The main idea is to approximate the probit-transform of the expected survival probability, i.e., $\Phi^{-1}(\mathbb{E}[S_{x,\tau}(u)|\kappa_\tau])$, where Φ^{-1} is the inverse of the standard normal distribution function, via the Taylor approximation. The probit-Taylor approximation is suitable for approximating $\mathbb{E}[S_{x,\tau}(u)|\kappa_\tau]$ because it assures that the approximated value is between 0 and 1. In addition, the probit function adds non-linearity to better approximate the expected survival probability. Although the original probit-Taylor approximation was not designed under the Lee-Carter model in Cairns (2011), it can be modified to work with the Lee-Carter model. Lemma 2.3 shows the probit-Taylor approximation for $\mathbb{E}[S_{x,\tau}(u)|\kappa_\tau]$ under the Lee-Carter model.

Lemma 2.3. *Suppose that the Lee-Carter model specified in equation* (3)–(4) *holds. For any age x, time τ, and duration u, a first-order probit-Taylor approximation for $\mathbb{E}[S_{x,\tau}(u)|\kappa_\tau]$ around an anchor scenario $\widetilde{\kappa}_\tau$ is given by*

$$\mathbb{E}[S_{x,\tau}(u)|\kappa_\tau] \approx \Phi\left(D_{x,\tau}(u) + D'_{x,\tau}(u)(\kappa_\tau - \widetilde{\kappa}_\tau)\right) \tag{17}$$

where $D_{x,\tau}(u) = \Phi^{-1}\left(\mathbb{E}\left[S_{x,\tau}(u)|\kappa_\tau = \widetilde{\kappa}_\tau\right]\right)$ and $D'_{x,\tau}(u) = \frac{d}{d\kappa_\tau}\Phi^{-1}\left(\mathbb{E}\left[S_{x,\tau}(u)|\kappa_\tau\right]\right)\Big|_{\kappa_\tau=\widetilde{\kappa}_\tau}$.

The probit-Taylor approximation (17) is useful for approximating $V(\kappa_\tau)$ for the temporary life annuity, but the quantities $D_{x,\tau}(u)$ and $D'_{x,\tau}(u)$ need to be estimated; see Appendix A for detailed derivations.

On the one hand, both approximation methods are computationally efficient because one only needs to estimate some relevant quantities via simulation once, then the values of $V(\kappa_\tau^{(i)})$ for all $i=1,\ldots,M$ can be approximated without any additional inner simulations. On the other hand, if estimated quantities are plugged into either approximation method, the resulting estimator for $V(\kappa_\tau)$ suffers both

approximation error and simulation error. The approximation error makes the valuation methods biased in general, and such a bias can only be reduced by adding higher order terms but cannot be completely eliminated in general. Also, the approximation errors tend to be larger for scenarios that are further away from the anchor scenario. If these scenarios happen to overlap with the tail scenarios that are important for estimating some tail risk measures, then the resulting risk estimator can be very poor. The simulation error adds variance to the approximated values of $V(\kappa_\tau^{(i)})$, so one needs to increase the number independent sample paths to reduce such variance.

3. Green nested simulation via likelihood ratios

In this section, we propose and analyze an efficient simulation procedure, called green nested simulation (GNS), for estimating $V(\kappa_\tau)$. The GNS procedure has similar convergence properties as the nested simulation procedure and requires similar low computations as the approximation methods.

3.1. The GNS procedure

Note that the time-τ value (2) can be written as

$$
\begin{aligned}
V(\kappa_\tau) = \mathbb{E}[H(\kappa_{\tau+})|\kappa_\tau] &= \int H(\kappa_{\tau+}) f(\kappa_{\tau+}|\kappa_\tau) d\kappa_{\tau+} \\
&= \int H(\kappa_{\tau+}) \frac{f(\kappa_{\tau+}|\kappa_\tau)}{g(\kappa_{\tau+})} g(\kappa_{\tau+}) d\kappa_{\tau+} \\
&= \mathbb{E}\left[H(\kappa_{\tau+}) \cdot W(\kappa_{\tau+}|\kappa_\tau)\right], \quad \kappa_{\tau+} \sim g(\kappa_{\tau+}),
\end{aligned}
\tag{18}
$$

where $g(\kappa_{\tau+})$ is a sampling density of the inner sample paths $\kappa_{\tau+}$ and $W(\kappa_{\tau+}|\kappa_\tau) = \frac{f(\kappa_{\tau+}|\kappa_\tau)}{g(\kappa_{\tau+})}$ is the likelihood ratio. Equation (18) is the well-known importance sampling identity and is the mathematical basis for our proposal. As in typical importance sampling studies, we assume that $g(\kappa_{\tau+}) > 0$ whenever $H(\kappa_{\tau+}) f(\kappa_{\tau+}|\kappa_\tau) > 0$ so that the likelihood ratio estimator $H(\kappa_{\tau+}) \cdot W(\kappa_{\tau+}|\kappa_\tau)$ is unbiased.

Inspired by (18), we propose the following *green nested simulation (GNS)* procedure:

1. Run the same outer-level simulation as the standard nested simulation to generate M independent realizations of κ_τ (i.e., $\kappa_\tau^{(1)}, \ldots, \kappa_\tau^{(M)}$) from the same density function $f(\kappa_\tau|\kappa_0)$.
2. Simulate $\widetilde{\Gamma}$ independent sample paths of $\kappa_{\tau+}$ (i.e., $\kappa_{\tau+}^{(1)}, \ldots, \kappa_{\tau+}^{(\widetilde{\Gamma})}$) according to a sampling mechanism whose sampling distribution is $g(\kappa_{\tau+})$. The sampling mechanism and sampling distribution in question will be discussed in Section 3.2.
3. For each outer scenario $\kappa_\tau^{(i)}$, $i = 1, \ldots, M$, estimate $V(\kappa_\tau^{(i)}) = \mathbb{E}[H(\kappa_{\tau+})|\kappa_\tau = \kappa_\tau^{(i)}]$ by the GNS estimator

$$
\widehat{V}_{\widetilde{\Gamma}}^{gns}(\kappa_\tau^{(i)}) = \frac{1}{\widetilde{\Gamma}} \sum_{j=1}^{\widetilde{\Gamma}} H(\kappa_{\tau+}^{(j)}) W(\kappa_{\tau+}^{(j)}|\kappa_\tau^{(i)}), \text{ where } W(\kappa_{\tau+}|\kappa_\tau^{(i)}) = \frac{f(\kappa_{\tau+}|\kappa_\tau^{(i)})}{g(\kappa_{\tau+})},
\tag{19}
$$

or by the self-normalized GNS estimator

$$
\widehat{V}_{\widetilde{\Gamma}}^{sn}(\kappa_\tau^{(i)}) = \frac{1}{\widetilde{\Gamma}} \sum_{j=1}^{\widetilde{\Gamma}} H(\kappa_{\tau+}^{(j)}) \bar{W}(\kappa_{\tau+}^{(j)}|\kappa_\tau^{(i)}),
\tag{20}
$$

where the self-normalized sample likelihood ratios are $\bar{W}(\kappa_{\tau+}^{(j)}|\kappa_\tau^{(i)}) = \frac{W(\kappa_{\tau+}^{(j)}|\kappa_\tau^{(i)})}{\frac{1}{\widetilde{\Gamma}} \sum_{\ell=1}^{\widetilde{\Gamma}} W(\kappa_{\tau+}^{(\ell)}|\kappa_\tau^{(i)})}$, $j = 1, \ldots, \widetilde{\Gamma}$. Self-normalization will be explained later.

4. Use the empirical distribution of the random sample $\{\widehat{V}_{\widetilde{\Gamma}}^{gns}(\kappa_\tau^{(i)}), i = 1, \ldots, M\}$ or $\{\widehat{V}_{\widetilde{\Gamma}}^{sn}(\kappa_\tau^{(i)}), i = 1, \ldots, M\}$ to estimate the risk measure $\rho(V_\tau)$ of interest.

The main benefit of the GNS procedure is its high computational efficiency, as it can be more accurate, less costly, or both, compared to the standard nested simulation. The GNS procedure requires a simulation budget of $\widetilde{\Gamma}$ inner sample paths. On the one hand, if one sets $\widetilde{\Gamma} = N$, then the GNS' simulation budget is a fraction, namely, $1/M$ of the standard nested simulation's budget. On the other hand, if one sets $\widetilde{\Gamma} = MN = \Gamma$ so that the simulation budgets of the GNS and standard nested simulation are the same, then for every scenario $\kappa_\tau^{(i)}$ the GNS estimators, self-normalized or not, utilize M times the number of inner paths as $\widehat{V}_N^{ns}(\kappa_\tau^{(i)})$ does and thus can be much more accurate than the latter. The consistency and high accuracy of the GNS estimator $\widehat{V}_{\widetilde{\Gamma}}^{gns}(\kappa_\tau^{(i)})$ is evidenced by Proposition 3.1. We denote convergence in probability, almost sure convergence, and convergence in distribution by $\xrightarrow{p}$, $\xrightarrow{a.s.}$ and $\xrightarrow{d}$, respectively.

Proposition 3.1. *Consider any given outer scenario κ_τ such that $V(\kappa_\tau)$ is defined (could be infinite unless stated otherwise). Assume that $g(\kappa_{\tau+})$ satisfies that $g(\kappa_{\tau+}) > 0$ whenever $H(\kappa_\tau, \kappa_{\tau+}) f(\kappa_{\tau+}|\kappa_\tau) \neq 0$. Then*

$$
\mathbb{E}\left[\widehat{V}_{\widetilde{\Gamma}}^{gns}(\kappa_\tau)\right] = V(\kappa_\tau),
\tag{21}
$$

$$
\widehat{V}_{\widetilde{\Gamma}}^{gns}(\kappa_\tau) \xrightarrow{p} V(\kappa_\tau) \text{ and } \widehat{V}_{\widetilde{\Gamma}}^{gns}(\kappa_\tau) \xrightarrow{a.s.} V(\kappa_\tau) \text{ as } \widetilde{\Gamma} \to \infty.
\tag{22}
$$

Moreover, if $\mathbb{V}\text{ar}[H(\kappa_{\tau+}) W(\kappa_{\tau+}|\kappa_\tau)] < \infty$, then

$$\frac{\widehat{V}_{\widetilde{\Gamma}}^{gns}(\kappa_\tau) - V(\kappa_\tau)}{\sqrt{\frac{\mathbb{V}\text{ar}[H(\kappa_{\tau^+})W(\kappa_{\tau^+}|\kappa_\tau)]}{\widetilde{\Gamma}}}} \xrightarrow{d} \mathcal{N}(0, 1) \ as \ \widetilde{\Gamma} \to \infty. \tag{23}$$

Equation (21) is a trivial consequence of Equation (18) and it shows that $\widehat{V}_{\widetilde{\Gamma}}^{gns}(\kappa_\tau)$ is an unbiased estimator of $V(\kappa_\tau)$. Equation (22) indicates that, in different modes of convergence, the GNS estimator can achieve an arbitrary accuracy as the simulation budget increases.

Equation (23) shows that the GNS estimator $\widehat{V}_{\widetilde{\Gamma}}^{gns}(\kappa_\tau)$ has a limiting normal distribution whose variance converges to zero at a rate of $\mathcal{O}(\widetilde{\Gamma}^{-1})$. The standard nested simulation estimator $\widehat{V}_N^{ns}(\kappa_\tau^{(i)})$ has similar properties, but with $\widetilde{\Gamma}$ replaced by N. In other words, by reusing only $\widetilde{\Gamma}$ inner paths, the GNS estimator converges as fast as a standard nested simulation estimator with $\widetilde{\Gamma}$ inner paths in *each of the M* outer scenarios; clearly the former has a much smaller simulation budget.

In the importance sampling literature, self-normalization is an enhancement technique that is commonly devised to reduce the variance of the importance sampling estimator. The likelihood ratio in a well-defined importance sampling estimator always has a unit expectation, i.e., $\mathbb{E}[W(\kappa_{\tau^+}|\kappa_\tau)] = 1$. However, for a random sample of inner sample paths, the sample average of the likelihood ratios may differ from 1. Self-normalization applies a ratio adjustment to the sample likelihood ratios such that the sample average of the self-normalized likelihood ratios equals 1. The self-normalized estimator $\widehat{V}_{\widetilde{\Gamma}}^{sn}(\kappa_\tau^{(i)})$ is biased in general, but the law of large numbers holds, as summarized in Lemma 3.2.

Lemma 3.2 (Paraphrase of Theorem 9.2 in Owen (2013)). *Consider any given outer scenario κ_τ such that $V(\kappa_\tau)$ is defined. Assume that $g(\kappa_{\tau^+})$ satisfies that $g(\kappa_{\tau^+}) > 0$ whenever $H(\kappa_\tau, \kappa_{\tau^+})f(\kappa_{\tau^+}|\kappa_\tau) \neq 0$. Then*

$$\widehat{V}_{\widetilde{\Gamma}}^{sn}(\kappa_\tau) \xrightarrow{p} V(\kappa_\tau) \ and \ \widehat{V}_{\widetilde{\Gamma}}^{sn}(\kappa_\tau) \xrightarrow{a.s.} V(\kappa_\tau) \ as \ \widetilde{\Gamma} \to \infty. \tag{24}$$

Lastly, when the risk factor κ_t is modeled by a Markovian process, the likelihood ratio can be calculated as

$$W(\kappa_{\tau^+}|\kappa_\tau) = \frac{f(\kappa_{\tau^+}|\kappa_\tau)}{g(\kappa_{\tau^+})} = \frac{f(\kappa_{\tau+1}|\kappa_\tau)f(\kappa_{\tau+2}|\kappa_{\tau+1})\cdots f(\kappa_T|\kappa_{T-1})}{g_{\tau+1}(\kappa_{\tau+1})f(\kappa_{\tau+2}|\kappa_{\tau+1})\cdots f(\kappa_T|\kappa_{T-1})} = \frac{f(\kappa_{\tau+1}|\kappa_\tau)}{g_{\tau+1}(\kappa_{\tau+1})}, \tag{25}$$

where $g_{\tau+1}(\kappa_{\tau+1})$ is the sampling distribution for the risk factor at time $\tau + 1$. Reducing the product of $(T - \tau)$ likelihood ratio calculations, i.e., $\frac{f(\kappa_{\tau^+}|\kappa_\tau)}{g(\kappa_{\tau^+})}$, to one, i.e., $\frac{f(\kappa_{\tau+1}|\kappa_\tau)}{g_{\tau+1}(\kappa_{\tau+1})}$, further reduces the computations needed for the GNS procedure.

3.2. Mixture sampling distribution

Compared to the standard nested simulation, the GNS offers the user the additional flexibility to select the sampling distribution $g(\kappa^+)$. For ease of exposition, in this study we simply use the standard nested simulation's sampling mechanism and argue that a mixture sampling distributions are valid for calculating the inner sample paths' likelihood ratios.

In the standard nested simulation, for each scenario $\kappa_\tau^{(i)}$, the sampling distribution for the corresponding inner sample paths is $f(\kappa_{\tau^+}|\kappa_\tau^{(i)})$. When reusing the j-th scenario's inner sample paths to estimate the i-th scenario's time-τ value, the likelihood ratio is $\frac{f(\kappa_{\tau^+}|\kappa_\tau^{(i)})}{f(\kappa_{\tau^+}|\kappa_\tau^{(j)})}$. This is similar to the "individual likelihood ratio (ILR)" estimator in Feng and Staum (2017), which has a poor performance. Intuitively, the ILR estimator has a large variance when the sampling scenario $\kappa_\tau^{(j)}$ and the target scenario $\kappa_\tau^{(i)}$ are significantly different, as then the likelihood ratio may have a large or even infinite variance (despite expectation still being 1).

The sampling mechanism in the standard nested simulation has another valid sampling distribution that leads to much better performance. Specifically, given M outer scenarios $\kappa_\tau^{(1)}, \ldots, \kappa_\tau^{(M)}$, the collective sample of all M scenarios' inner sample paths, i.e., $\{\kappa_{\tau^+}^{(ij)}, j = 1, \ldots, N, i = 1, \ldots, M\}$, can be viewed as a stratified sample of the mixture distribution

$$g(\kappa_{\tau^+}) = \frac{1}{M} \sum_{i=1}^M f(\kappa_{\tau^+}|\kappa_\tau^{(i)}). \tag{26}$$

The mixture distribution (26) weights the M conditional distributions equally because the same number of inner sample paths are generated in each outer scenario in a standard nested simulation. This mixture distribution can be employed in the GNS procedure with or without self-normalization. We adopt the mixture sampling distribution in our numerical studies.

The mixture sampling distribution can be mathematically justified (Veach and Guibas, 1995; Feng and Staum, 2017) and the resulting GNS estimator is unbiased. That is, noting that $\kappa_{\tau^+}^{(ij)} \overset{i.i.d.}{\sim} f(\kappa_{\tau^+}|\kappa_\tau^{(i)})$ for $j = 1, \ldots, N$ and $i = 1, \ldots, M$, for any scenario κ_τ we have

$$\begin{aligned}
\mathbb{E}\left[\widehat{V}_\Gamma^{gns}(\kappa_\tau)\right] &= \mathbb{E}\left[\frac{1}{MN} \sum_{i=1}^M \sum_{j=1}^N H(\kappa_{\tau^+}^{(ij)})\frac{f(\kappa_{\tau^+}|\kappa_\tau)}{g(\kappa_{\tau^+})}\right] \\
&= \frac{1}{N} \sum_{j=1}^N \frac{1}{M} \sum_{i=1}^M \mathbb{E}\left[H(\kappa_{\tau^+}^{(ij)})\frac{f(\kappa_{\tau^+}^{(ij)}|\kappa_\tau)}{g(\kappa_{\tau^+})}\right], \quad \kappa_{\tau^+}^{(ij)} \sim f(\kappa_{\tau^+}|\kappa_\tau^{(i)}) \\
&= \frac{1}{N} \sum_{j=1}^N \frac{1}{M} \sum_{i=1}^M \int H(\kappa_{\tau^+})\frac{f(\kappa_{\tau^+}|\kappa_\tau)}{g(\kappa_{\tau^+})} f(\kappa_{\tau^+}|\kappa_\tau^{(i)})d\kappa_{\tau^+}
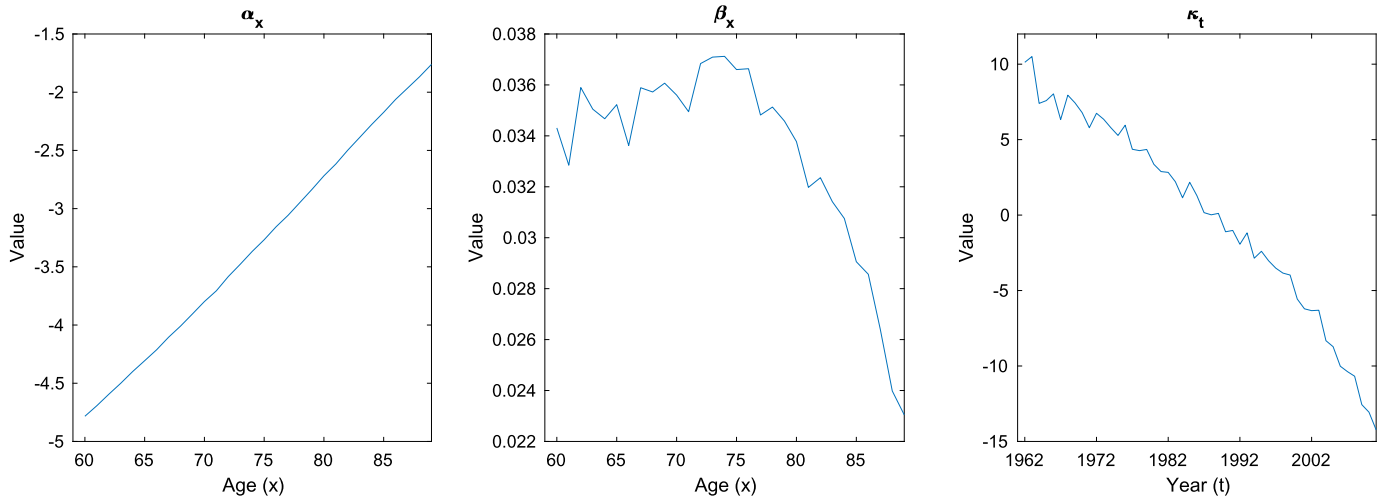\end{aligned}$$

Fig. 1. Estimates of α_x, β_x and κ_t in the Lee-Carter model.

$$= \frac{1}{N} \sum_{j=1}^{N} \int H(\kappa_{\tau+}) \frac{\frac{1}{M} \sum_{i=1}^{M} f(\kappa_{\tau+}|\kappa_\tau^{(i)})}{g(\kappa_{\tau+})} f(\kappa_{\tau+}|\kappa_\tau) d\kappa_{\tau+}$$

$$= \frac{1}{N} \sum_{j=1}^{N} \int H(\kappa_{\tau+}) f(\kappa_{\tau+}|\kappa_\tau) d\kappa_{\tau+} = V(\kappa_\tau).$$

This stratified implementation of mixture sampling is also studied by Hesterberg (1988); Veach and Guibas (1995); Broadie and Glasserman (2004); Feng and Staum (2017); Dong et al. (2018), and Elvira et al. (2019). Elvira et al. (2019) show that stratified implementation is statistically valid and produces more accurate estimators than a non-stratified implementation. The stratified implementation of mixture sampling is also referred to as the balance heuristic by Hesterberg (1988) and the mixture likelihood ratio (MLR) estimator by Feng and Staum (2017) and Dong et al. (2018). These researchers also find that the mixture sampling distribution (26) produces highly accurate estimators.

3.3. Remark

In some risk management applications, valuation of derivative securities is performed under a risk-neutral measure. For such applications, the outer scenarios κ_τ and the inner sample paths $\kappa_{\tau+}$ should be simulated under the real-world probability measure $\mathbb{P}$ and a corresponding risk-neutral probability measure $\mathbb{Q}$, respectively. Our proposed green nested simulation approach is applicable to this setting, as long as the risk-neutral density $f^{\mathbb{Q}}(\kappa_{\tau+}|\kappa_\tau)$ exists and the sampling distribution g satisfies the absolute continuity condition.

4. Numerical case studies

In this section we conduct three case studies, one for each type of mortality-linked securities discussed in Section 2.3, to demonstrate the efficiency and accuracy of the proposed GNS procedure in comparison to the standard nested simulation and various approximation methods. In what follows, we assume that the current time point is 0, the time-to-maturity is T years, the risk horizon is τ years, and the discount rate r is 3%.

To fit the Lee-Carter model, we use mortality data from the female population of England and Wales, over an age range of 60 to 89 and a sample period of 1962 to 2011. The data is obtained from the Human Mortality Database. The parameters of the Lee-Carter model are estimated using the Poisson maximum likelihood method (Brouhns et al., 2002a). The resulting estimates of the age-specific parameters α_x and β_x and the risk factor κ_t are reported in Fig. 1. The estimates of θ and σ_ϵ in the process for the risk factor are -0.4971 and 0.7467, respectively. Given the estimate of κ_0 (-14.2328), sample paths of κ_t beyond time 0 can be simulated readily.

In each case study, we compare the accuracies of different valuation methods for fixed and random scenarios. Let $\widehat{V}(\kappa_\tau)$ be an estimator of $V(\kappa_\tau)$ based on one of the valuation methods. For a fixed scenario κ_τ, one way to assess the accuracy of $\widehat{V}(\kappa_\tau)$ is its 95% confidence interval, i.e., the width between the 2.5%- and the 97.5%-tiles of $\widehat{V}(\kappa_\tau)$ for a fixed scenario κ_τ and random inner sample paths. The confidence interval width mainly shows the variability of the estimator caused by the inner path randomness.

The mean square error

$$MSE(\kappa_\tau) = \mathbb{E}\left[\left.\left(\widehat{V}(\kappa_\tau) - V(\kappa_\tau)\right)^2\right| \kappa_\tau\right]$$

is another popular error measure that accounts for both the variance and the bias of the estimator. The value of $MSE(\kappa_\tau)$ reflects the stochasticity of the inner scenarios for a given κ_τ. However, this measure does not consider the stochasticity of the outer scenarios, resulting from the randomness in κ_τ given $\mathcal{F}_0$. To incorporate the stochasticity of the outer scenarios, we suggest comparing the integrated mean squared error (IMSE) for different valuation methods:

$$IMSE = \mathbb{E}\left[\left(\widehat{V}(\kappa_\tau) - V(\kappa_\tau)\right)^2\right] = \mathbb{E}\left[MSE(\kappa_\tau)\right], \tag{27}$$
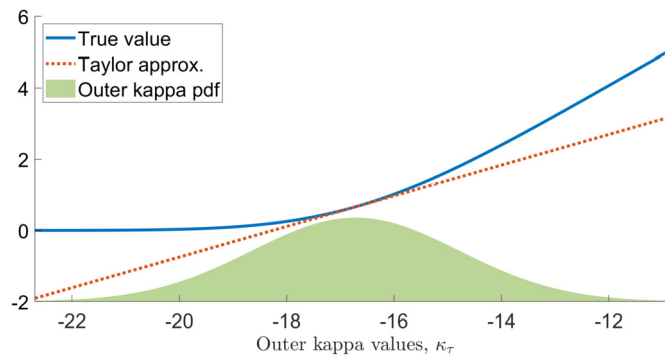
Fig. 2. Problem settings for risk measurement of a K-call.

where the expectation is taken with respect to the distribution of κ_τ given $\mathcal{F}_0$. In some applications, the IMSE itself can be a risk measure $\rho(V(\kappa_\tau))$ of interest. Similar to the MSE, the IMSE can be decomposed as the sum of the integrated variance and the integrated squared bias.

In the simulation experiments, we simulate $M = 10^3$ outer scenarios from $\kappa_\tau^{(i)} \sim \mathcal{N}(\kappa_0 + \tau\theta, \tau\sigma_\epsilon^2)$, $i = 1, \ldots, M$. We then, for each simulated outer scenario $\kappa_\tau^{(i)}$, estimate $V(\kappa_\tau^{(i)})$ via different valuation methods. For better uniformity and more accurate error estimates, instead of randomly simulating from $\mathcal{N}(\kappa_0 + \tau\theta, \tau\sigma_\epsilon^2)$, we set the 10^3 outer scenarios to 10^3 equally-spaced quantiles of $\mathcal{N}(\kappa_0 + \tau\theta, \tau\sigma_\epsilon^2)$. For the Taylor and probit-Taylor approximations, the anchor scenario is $\widetilde{\kappa} = \mathbb{E}[\kappa_\tau] = \kappa_0 + \tau\theta$. To estimate the MSEs and IMSEs, for each outer scenario $\kappa_\tau^{(i)}$ and each valuation method we repeatedly and independently estimate $V(\kappa_\tau^{(i)})$ for $R = 10^3$ times. The IMSE is estimated by

$$\widehat{IMSE} = \frac{1}{M} \sum_{i=1}^{M} \left[\frac{1}{R} \sum_{r=1}^{R} \left(\widehat{V}_{(r)}(\kappa_\tau^{(i)}) - V(\kappa_\tau^{(i)}) \right)^2 \right], \tag{28}$$

where $\widehat{V}_{(r)}(\kappa_\tau^{(i)})$ is an estimate for $V(\kappa_\tau^{(i)})$ in the r-th macro replication. When the closed-form formula for $V(\kappa_\tau^{(i)})$ is not available, it is replaced by an accurate Monte Carlo estimate with 10^7 inner sample paths.

The valuation methods considered in our case studies are outlined below.

- Standard nested simulation: For this method, we consider three different numbers of inner simulations: 1, 10 and 100. As there are $M = 10^3$ outer scenarios, these cases correspond to simulation budgets of 10^3, 10^4, and 10^5, respectively.
- Taylor approximation: For this method, to emulate practical cases, the value function $V(\widetilde{\kappa}_\tau)$ and its derivative $V'(\widetilde{\kappa}_\tau)$ are estimated via inner simulations. For fairness of comparison with the other methods, we consider 10^3, 10^4, and 10^5 inner sample paths to estimate these quantities.
- GNS procedure: For this method, all of the inner sample paths are generated by the same way as in the standard nested simulation. The mixture distribution (26) is used as the sampling distribution in the denominator of the likelihood ratio. Both the regular and the self-normalized GNS estimators are considered.

4.1. Case study 1: K-call

Consider a \$1 notional K-call option that matures in $T = 10$ years and has a strike set to the expected value at maturity, i.e., $K = \mathbb{E}[\kappa_T | \kappa_0] = -19.20$. The risk horizon of interest is $\tau = 5$ years. The K-call's payoff is simple so a closed-form formula for $V(\tau)$ is available under the Lee-Carter model.

Fig. 2 summarizes this case study's settings. The outer scenario's density is shown as the shaded bell curve; the endpoints are the 0.1%-tile and 99.9%-tile of the outer distribution. The closed-form value and the Taylor approximation of $V(\kappa_\tau)$ are plotted as a solid line and a dotted line, respectively. For the Taylor approximation, the values of $V(\widetilde{\kappa})$ and $V'(\widetilde{\kappa})$ are analytically calculated using closed-form formulas (see Proposition 2.2). Note that $V(\kappa_\tau)$ is a convex function of κ_τ for the K-call considered, and hence the (first-order) Taylor approximation is biased low even without any inner simulation error.

Fig. 3 depicts the 95% confidence bands for different valuation methods; the color-coding indicates the different simulation budgets. We see that, as the simulation budget increases, all confidence bands narrow. The standard nested simulation (panel (a)) and the two GNS procedures (panels (c) and (d)) have confidence bands centered around the true value. But the confidence bands for the Taylor approximation (panel (b)) are centered around the accurate Taylor approximation without simulation error, which is below the true value. This shows that the Taylor approximation suffers both approximation errors and simulation errors. Moreover, increasing the simulation budget can reduce the simulation error, but the approximation error persists no matter how many inner simulations are deployed. Panels (a), (c) and (d) also show, at least graphically, that the two GNS estimators are more accurate than the standard nested simulation. Lastly, comparing panel (c) and panel (d), we see that self-normalization significantly reduces the variability of the GNS estimator.

We also see in Fig. 3 that the confidence bands for both GNS procedures (panels (c) and (d)) are wider as the outer kappa values become higher. The increase in width is because the outer kappa values concentrate around the mean of the outer distribution, as shown in Fig. 2, so that the mixture sampling distribution also centers around the same mean. As a result, the standard errors for the outer kappa values that are far away from the center of the mixture sampling distribution are high. Nonetheless, over the range of outer kappa values shown (which spans from the 0.1%-tile to the 99.9%-tile of the outer distribution), the confidence bands obtained from the GNS procedure are narrower than those generated from the standard nested simulation.
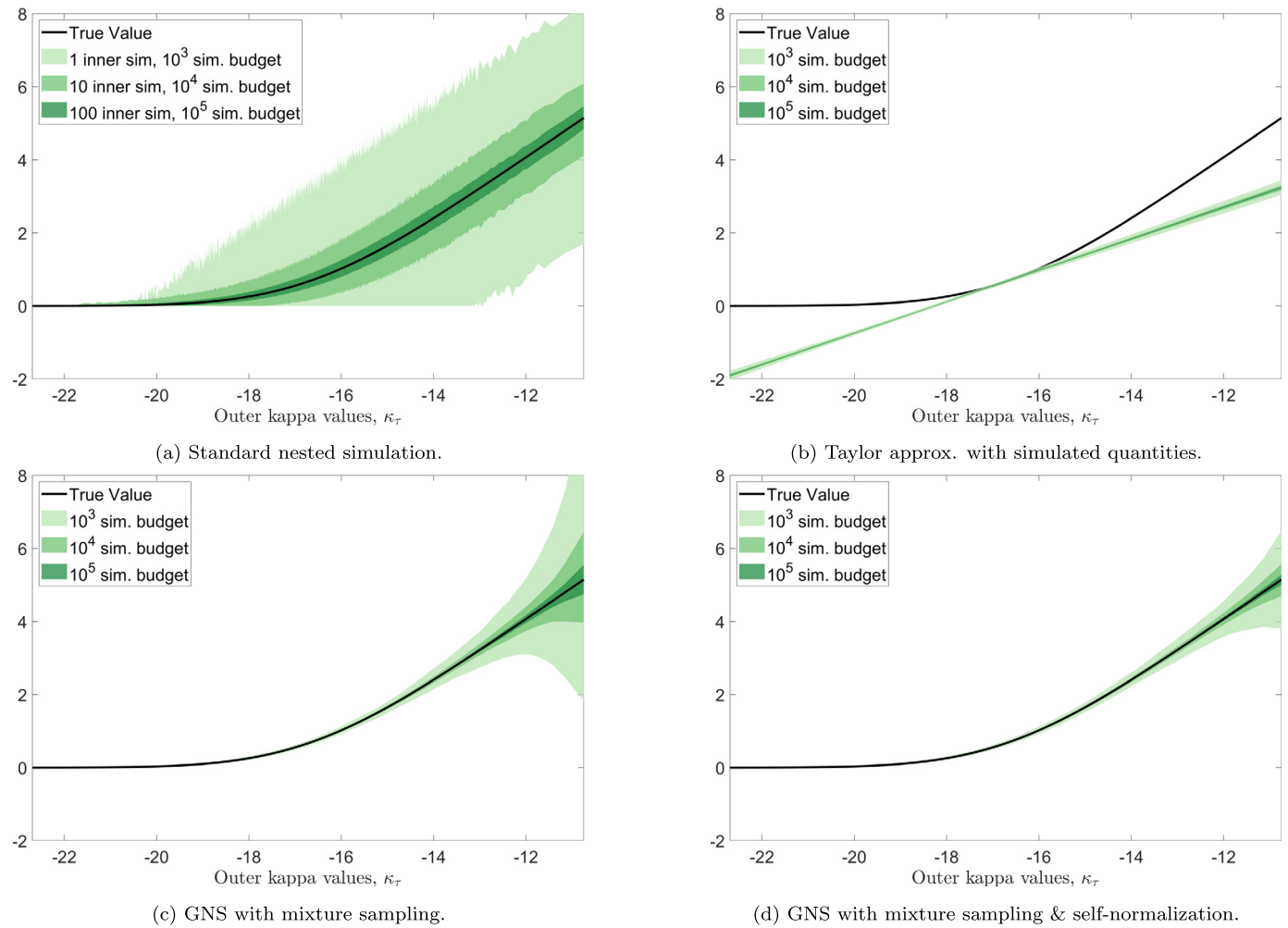
(a) Standard nested simulation.

(b) Taylor approx. with simulated quantities.

(c) GNS with mixture sampling.

(d) GNS with mixture sampling & self-normalization.

Fig. 3. 95% confidence bands for estimating $V(\kappa_\tau)$ for different valuation methods, K-call example.

Table 1
Estimated IMSEs for the K-option case study.

Case study	K-option		
Simulation budget	10^3	10^4	10^5
Standard nested sim.	1.08	1.08×10^{-1}	1.08×10^{-2}
Taylor approx.	1.84×10^{-1}	1.83×10^{-1}	1.83×10^{-1}
Green nested sim.	1.55×10^{-2}	1.55×10^{-3}	1.49×10^{-4}
GNS, self-normalized	4.47×10^{-3}	4.92×10^{-4}	4.58×10^{-5}

Fig. 4 depicts, in log-log scale, the estimated IMSEs for different valuation methods versus the simulation budget. The values of the IMSEs in Fig. 4 are also summarized in Table 1 for quantitative comparisons. We see that, for any given simulation budget, the IMSEs of the two GNS estimators are significantly smaller than those of the standard nested simulation and the Taylor approximation. For example, the self-normalized GNS estimator's IMSE is more than 200 times smaller than the standard nested simulation's. Moreover, we see that the GNS estimators' IMSEs decrease as quickly as that of the standard nested simulation estimator; the slopes for their IMSEs are close to -1 in Fig. 4. This outcome is expected because these procedures produce (asymptotically) unbiased estimators so their MSEs coincide with their variances, which converge at the rate of $\mathcal{O}(\Gamma^{-1})$. We also see that the Taylor approximation's IMSE barely decreases as the simulation budget increases. This indicates that the IMSEs are mostly contributed by the biases due to approximation errors, which cannot be reduced by increasing simulation budget. With a small simulation budget (10^3), the self-normalized GNS estimator's IMSE is about 40 times smaller than that of the Taylor approximation. When the simulation budget is large (10^5), the self-normalized GNS estimator's IMSE is almost 4,000 times smaller. Lastly, the self-normalized GNS estimator outperforms the regular GNS estimator for all of the simulation budgets considered.

For the reader's information, we repeated the experiment with $M = 100$ outer scenarios and the same range of simulation budgets as that for Fig. 4. The result is summarized graphically in Fig. 5, which should be interpreted in the same matter as Fig. 4. Two observations are made through the comparison between Figs. 4 and 5. First, for the standard nested simulation, the IMSE is almost 10 times smaller if the number of outer scenarios M is reduced from 1000 to 100 while the simulation budget remains unchanged. This outcome is because as M is reduced by 10 times (given a certain simulation budget), the number of inner replications N for each outer scenario is increased by 10 times and consequently the IMSE is improved at a similar rate. On the other hand, there is no change to the IMSEs for the Taylor
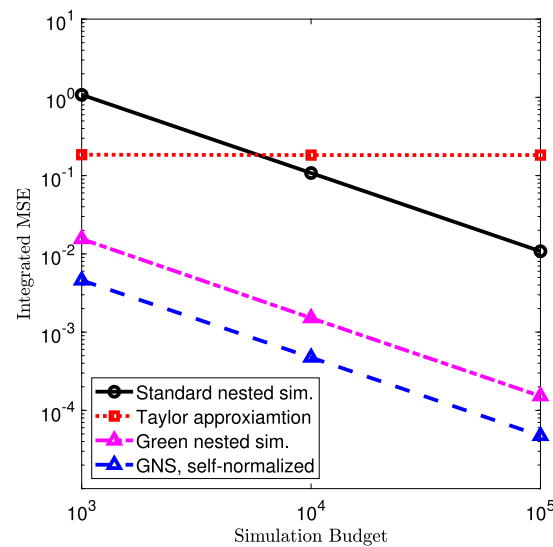
Fig. 4. Estimated IMSEs for different valuation methods and simulation budgets when the number of outer simulations is set to $M = 1000$, K-call example.
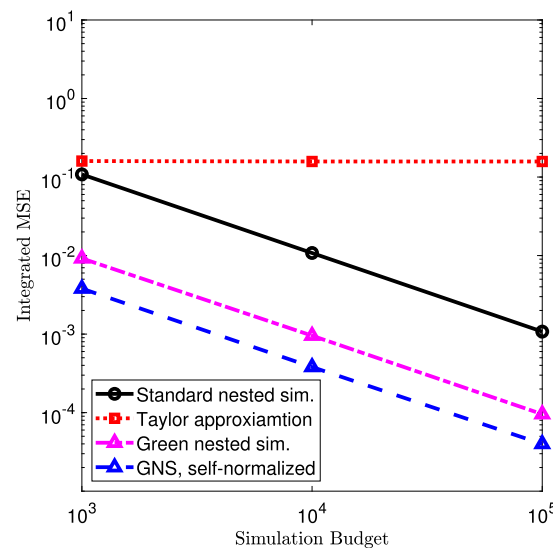

Fig. 5. Estimated IMSEs for different valuation methods and simulation budgets when the number of outer simulations is set to $M = 100$, K-call example.

approximation and GNS procedures when the number of outer scenarios M is reduced and the simulation budget remains fixed. This outcome is because the IMSEs of these procedures depend on the total simulation budget rather than the number of inner replications.

In conclusion, we recommend using the self-normalized GNS procedure in practical applications. In the next two case studies, we will neglect the regular GNS procedure and only focus on the effectiveness of the self-normalized GNS procedure.

4.2. Case study 2: q-call-spread

Consider a q-call-spread with a reference age of $x = 60$ and a time-to-maturity of $T = 10$ years at time 0. The attachment and exhaustion points are set at the 5%- and 95%-tiles of the underlying probability of death of the call spread, i.e., $AP = 3.703 \times 10^{-2}$ and $EP = 5.037 \times 10^{-2}$, respectively. The risk horizon of interest is $\tau = 5$ years. As there is no closed-form formula for $V(\kappa_\tau)$, inner simulation is necessary.

Fig. 6 depicts the settings of this case study. The payoff at maturity of the q-call-spread has two kink points, i.e., the attachment and the exhaustion points, and therefore the curve of its time-τ values is "S"-shaped. Consequently, the Taylor approximation underestimates $V(\kappa_\tau)$ if κ_τ is smaller than the anchor scenario $\widetilde{\kappa}$, and overestimates $V(\kappa_\tau)$ if otherwise.

Fig. 7 shows the 95% confidence bands for estimating $V(\kappa_\tau)$ by the standard nested simulation (panel (a)), Taylor approximation (panel (b)), and the self-normalized GNS estimator (panel (c)). The Taylor approximation in Fig. 7b uses estimated $V(\widetilde{\kappa}_\tau)$ and $V'(\widetilde{\kappa}_\tau)$ (see Appendix A), which means it suffers both approximation error (bias) and simulation error (variance). Comparing panel (a) and panel (c), we see that the self-normalized GNS is significantly more accurate than the standard nested simulation. We also see that compared to the Taylor approximation (panel (a)), the self-normalized GNS estimator (panel (c)) has a high variance for scenarios that are far from the mean of the outer scenario distribution (e.g., extreme values on either side in this 1-dimensional example); however, the Taylor approximation showed high bias for the extreme outer values.
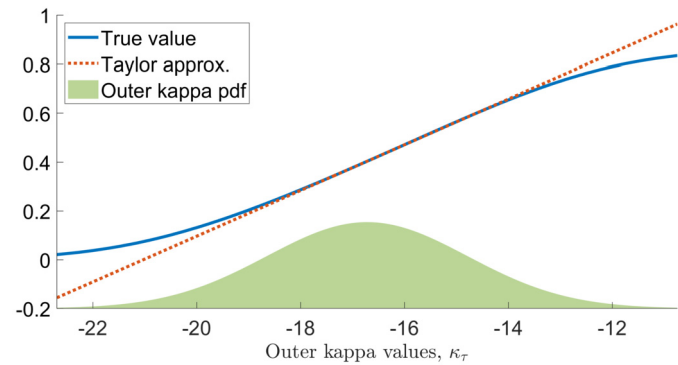
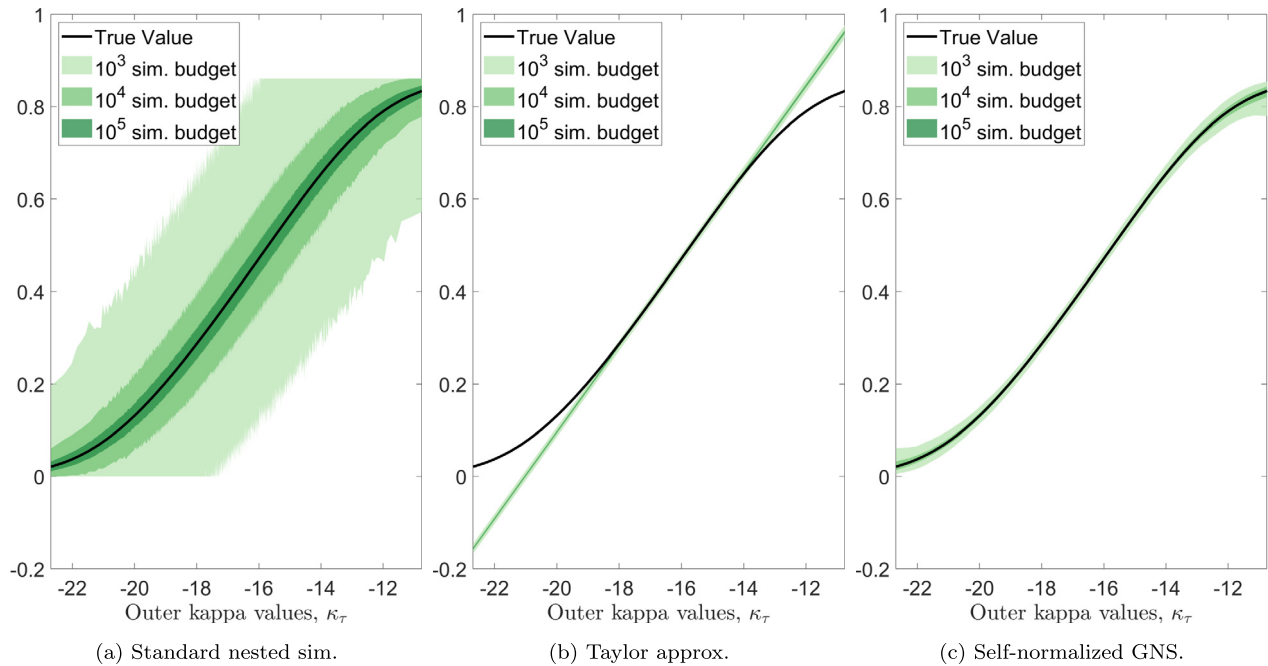**Fig. 6.** Problem settings for risk measurement of a *q*-call-spread.

Fig. 7. 95% confidence bands for estimating $V(\kappa_\tau)$ for different valuation methods, *q*-call-spread example.

Table 2
Estimated IMSEs for the q-call-spread case study.

Case study	q-Call-Spread		
Simulation budget	10^3	10^4	10^5
Standard nested sim.	2.90×10^{-2}	2.91×10^{-3}	2.90×10^{-4}
Taylor approx	4.01×10^{-4}	3.69×10^{-4}	3.66×10^{-4}
GNS, self-normalized	7.35×10^{-5}	7.27×10^{-6}	7.63×10^{-7}

Fig. 8a depicts the IMSEs for this case study. The numerical values are reported in Table 2. Note that, similar to MSE, the IMSE accounts for both the biases and variances for different valuation methods. Firstly, from Fig. 8a, we can draw similar conclusions as those from Fig. 4 for *K*-call: (1) the self-normalized GNS estimator is orders of magnitudes more accurate than the standard nested simulation and the Taylor approximation, and (2) the self-normalized GNS estimator's IMSE converges as quickly as that for the standard nested simulation. In addition, Fig. 8a shows some merits of the Taylor approximation; it can achieve a similar level of accuracy as the standard nested simulation, but with only a fraction of the simulation budget. Nonetheless, for different simulation budgets, the self-normalized GNS estimator's IMSE is significantly smaller than that of the other two methods. More importantly, as the simulation budget increases, the Taylor approximation's IMSE is stagnant while the GNS estimator's IMSE converges as quickly as the standard nested simulation. When the simulation budget is large (10^5), the IMSE of the self-normalized GNS estimator is about 400 and 500 times smaller than that of the standard nested simulation and the Taylor approximation, respectively.

4.3. Case study 3: temporary life annuity

In this case study, we consider a $T = 30$ year temporary life annuity that is issued at time 0 to an insured aged $x_0 = 60$. The risk horizon of interest is $\tau = 10$ years. At time $\tau = 10$, assuming that the insured has survived to age $x_0 + \tau = 70$, the remaining annuity
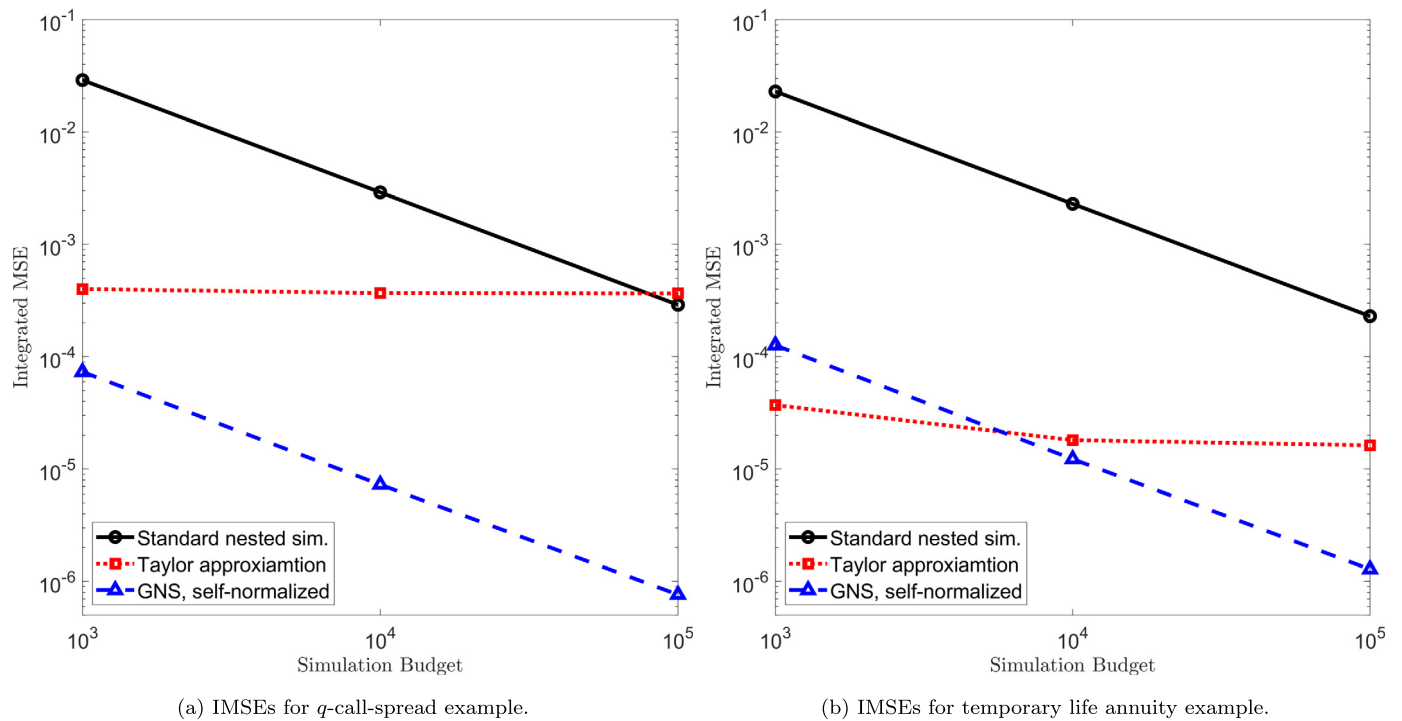
(a) IMSEs for q-call-spread example.

(b) IMSEs for temporary life annuity example.

Fig. 8. Estimated IMSEs for different valuation methods and simulation budgets, q-call-spread and temporary life annuity examples.
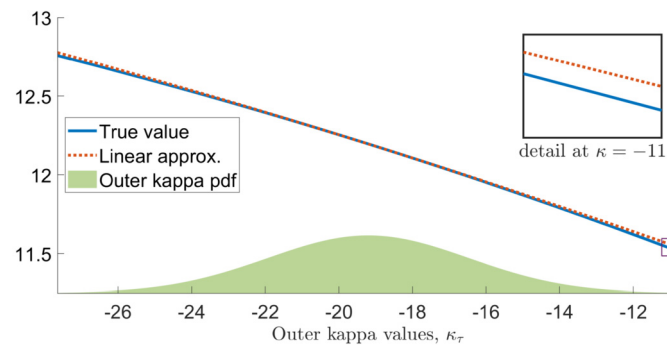

Fig. 9. Problem settings for risk measurement of a temporary life annuity.

liability is a $T - \tau = 20$ year temporary life annuity. There is no closed-form formula for $V(\kappa_\tau)$ of a 20 year temporary life annuity, because of the complexity of an annuity's payoff in relation with κ_τ; the conditional expectation of a survival probability cannot be solved analytically. As discussed in Section 2.4.3, the conditional expectations of the survival probabilities involved in an annuity can be approximated by the probit-Taylor approximation (17) in Lemma 2.3. For illustration purposes, we set the probit-Taylor approximation around the anchor scenario $\widetilde{\kappa}_\tau = \mathbb{E}[\kappa_{10}|\kappa_0] = -19.20$.

Fig. 9 depicts the settings for this case study. Unlike the Taylor approximations in Figs. 2 and 6, which are linear, the probit-Taylor approximation in Fig. 9 is slightly non-linear. As a result, it approximates $V(\kappa_\tau)$ for the temporary life annuity quite well.

Fig. 10 shows the 95% confidence bands for estimating $V(\kappa_\tau)$ by the standard nested simulation (panel (a)), Taylor approximation (panel (b)), and the self-normalized GNS estimator (panel (c)). We see from Fig. 10b that the bias and variance of the probit-Taylor approximation are both small. We also see from Fig. 10c that the self-normalized GNS estimator is clearly more accurate than the standard nested simulation, but its variance around extreme outer scenario values are higher than the variance for the probit-Taylor approximation. We shall examine the trade-off between bias and variance in more detail in the next paragraph using Table 3.

Fig. 8b and Table 3 graphically and numerically summarize the IMSEs of this case study, respectively. It is clear that both the GNS estimator and the probit-Taylor approximation have IMSEs that are orders of magnitudes smaller than that of the standard nested simulation. Moreover, when the simulation budget is small (10^3), the probit-Taylor approximation has small approximation and simulation errors, resulting in a smaller IMSE than the GNS estimator. However, as the simulation budget increases, the GNS estimator's IMSE quickly decreases while the probit-Taylor approximation's IMSE only decreases slightly. When the simulation budget is large (10^5), the self-normalized GNS estimator's IMSE is over 12 times smaller than the probit-Taylor approximation's; the gap will continue to widen as the simulation budget increases.

In summary, our three case studies show that the proposed GNS procedure can produce accurate risk estimators for different types of mortality-linked securities. Measured by IMSE, the self-normalized GNS estimator is orders of magnitudes more accurate than the standard nested simulation, and its IMSE converges to zero as fast as the latter. The GNS procedure is also more generally applicable and has a high accuracy for most simulation budgets. In contrast, the approximation method demands customized construction and derivation for
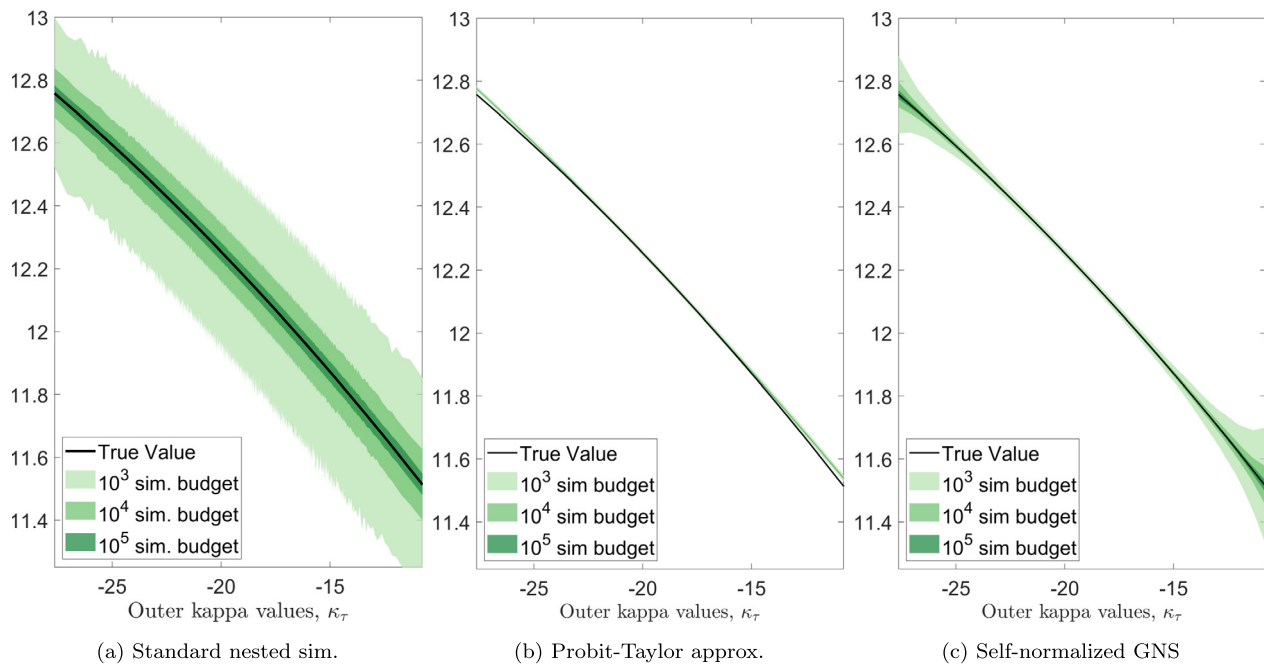
Fig. 10. 95% confidence bands for estimating $V(\kappa_\tau)$ for different valuation methods, temporary life annuity example.

Table 3
Estimated IMSEs for the temporary life annuity case study.

Case study	Temporary Life Annuity		
Simulation budget	10^3	10^4	10^5
Standard nested sim.	2.30×10^{-2}	2.30×10^{-3}	2.30×10^{-4}
(Probit-)Taylor approx	3.71×10^{-5}	1.81×10^{-5}	1.63×10^{-5}
GNS, self-normalized	1.27×10^{-4}	1.23×10^{-5}	1.28×10^{-6}

different types of mortality-linked securities. The accuracy of the approximation method also varies and suffers significantly when the security's payoff is non-linear.

5. Concluding remarks

In this study we propose, analyze, and test an efficient simulation procedure, the *green nested simulation (GNS)*, for nested risk estimation problems in the context of mortality-linked securities. Compared to the standard nested simulation, the GNS procedure produces more accurate estimates with the same simulation budget, and can be expected to significantly reduce the computations needed to achieve a prescribed accuracy. Approximation methods such as the Taylor and probit-Taylor approximations are biased so their IMSEs do not converge to zero in general. In contrast, the GNS is unbiased, or asymptotically so, and thus the resulting estimator can achieve an arbitrary level of accuracy when a sufficient simulation budget is given. Our numerical studies show that the GNS estimator's IMSE converge as fast as the standard nested simulation's. Moreover, to achieve a high accuracy, the approximation methods require customized derivations for different securities and payoff structures. The GNS procedure, in comparison, requires no such customization.

In a more practical setting, the quantity of interest may involve individuals at different ages; for instance, a portfolio of life annuities with a dispersed age profile. As long as the ages involved are covered by the age range to which the assumed mortality model is fitted, the GNS method proposed in this paper is still applicable. The computational saving for such applications may be even higher than that demonstrated in this paper, because different age groups share the same likelihood ratio calculations.

We also remark that the proposed GNS method can be extended to include the situation when we are interested in the values of a mortality-related security, liability or portfolio at various future time points. Specifically, if the repeated experiments are sufficiently similar (or even identical except for some initial inputs), then one might be able to design a new green simulation procedure that reuses simulation outputs spatially and temporally (see, e.g., how the GNS procedure in Feng and Staum (2017) reuses outputs in repeated experiments).

To focus on the uncertainty surrounding mortality dynamics, this paper does not consider any other source of uncertainty. In future research, it would be interesting to include other risk factors such as interest rates and stock indices into our simulation framework, so that it can be applicable to a broader range of insurance products including variable annuities and equity-indexed annuities.

Declaration of competing interest

The authors declare that there is no competing interest.

Acknowledgement

Appendix A. Pathwise gradient estimators for $V(\kappa_\tau)$

In this appendix, we derive the pathwise gradient estimators for $V(\kappa_\tau)$. These estimators are used in the implementation of the approximation methods discussed in Section 2.4.

The following representation of the terminal period effect κ_T under the Lee-Carter model will be useful in this appendix:

$$\kappa_T = \kappa_\tau + Z_{\tau,T},$$

where $Z_{\tau,T} \sim \mathcal{N}((T-\tau)\theta, (T-\tau)\sigma_\epsilon^2)$ and $\tau \leq T$.

For a K-call, the derivative of $V(\kappa_\tau)$ with respect to κ_τ is

$$V'(\kappa_\tau) = \frac{d\mathbb{E}\left[e^{-r(T-\tau)}(\kappa_T - K)^+|\kappa_\tau\right]}{d\kappa_\tau} = e^{-r(T-\tau)}\mathbb{E}\left[\frac{d(\kappa_\tau + Z_{\tau,T} - K)^+}{d\kappa_\tau}\Big|\kappa_\tau\right]$$

$$= e^{-r(T-\tau)}\mathbb{E}\left[\mathbf{1}_{\{\kappa_\tau + Z_{\tau,T} > K\}}|\kappa_\tau\right],$$

where the equalities hold by verifying the unbiasedness conditions in Section 7.2.2 in Glasserman (2004). One can then estimate $V'(\widetilde{\kappa}_\tau)$ via simulation by

$$\widehat{V}'_N(\widetilde{\kappa}_\tau) = \frac{e^{-r(T-\tau)}}{N}\sum_{j=1}^{N}\mathbf{1}_{\{\widetilde{\kappa}_\tau + Z_{\tau,T}^{(j)} > K\}},$$

where $Z_{\tau,T}^{(j)} \sim \mathcal{N}((T-\tau)\theta, (T-\tau)\sigma_\epsilon^2)$, $j = 1, \ldots, N$. The subscript N in $\widehat{V}'_N(\widetilde{\kappa}_\tau)$ indicates the number of independent inner sample paths simulated.

In Section 2.3 we see that the payoffs of some longevity-linked securities, such as q-spreads and temporary life annuities, depend on κ_t through the survival probabilities $S_{x,t}(u)$ for some x, t and u. Recall from equation (7) that the survival probability under the Lee-Carter model is $S_{x,t}(u) = \exp\left(-\sum_{s=1}^{u}\exp(\alpha_{x+s-1} + \beta_{x+s-1}\kappa_{t+s})\right)$. It follows that the derivative of $S_{x,t}(u)$ with respect to κ_t is

$$\frac{d}{d\kappa_t}S_{x,t}(u) = S_{x,t}(u) \cdot \left(-\sum_{s=1}^{u}\beta_{x+s-1} \cdot e^{\alpha_{x+s-1} + \beta_{x+s-1}\kappa_{t+s}}\right). \tag{A.1}$$

Using the derivative in (A.1) and the chain rule, one can estimate the derivative of $V(\kappa_\tau)$ with respect to κ_τ for longevity-linked securities that depend on κ_t through $S_{x,t}(u)$. For example, the derivative of $V(\kappa_\tau)$ with respect to κ_τ for a q-call-spread is

$$V'(\kappa_\tau)$$
$$= \frac{e^{-r(T-\tau)}}{EP - AP} \cdot \frac{d}{d\kappa_\tau}\left(\mathbb{E}[(q_{x,T} - AP)^+|\kappa_\tau] - \mathbb{E}[(q_{x,T} - EP)^+|\kappa_\tau]\right)$$
$$= \frac{e^{-r(T-\tau)}}{EP - AP} \cdot \left(\mathbb{E}\left[\frac{d}{d\kappa_\tau}(1 - S_{x,T-1}(1) - AP)^+\Big|\kappa_\tau\right] - \mathbb{E}\left[\frac{d}{d\kappa_\tau}(1 - S_{x,T-1}(1) - EP)^+\Big|\kappa_\tau\right]\right)$$
$$= \frac{e^{-r(T-\tau)}}{EP - AP} \cdot \left(\mathbb{E}\left[\mathbf{1}_{\{1-EP > S_{x,T-1}(1)\}}\frac{dS_{x,T-1}(1)}{d\kappa_\tau}\Big|\kappa_\tau\right] - \mathbb{E}\left[\mathbf{1}_{\{1-AP > S_{x,T-1}(1)\}}\frac{dS_{x,T-1}(1)}{d\kappa_\tau}\Big|\kappa_\tau\right]\right),$$

where

$$\frac{dS_{x,T-1}(1)}{d\kappa_\tau} = -S_{x,T-1}(1) \cdot \beta_x \cdot e^{\alpha_x + \beta_x(\kappa_\tau + Z_{\tau,T})}.$$

To estimate $V'(\widetilde{\kappa}_\tau)$, one can again use simulation to compute the two expectations in $V'(\kappa_\tau)$ and in turn obtain $\widehat{V}'_N(\widetilde{\kappa}_\tau)$.

Lastly, we consider a temporary life annuity, whose time-τ value is

$$V(\kappa_\tau) = \sum_{u=1}^{T-\tau} e^{-ru}\mathbb{E}[S_{x_0+\tau,\tau}(u)|\kappa_\tau].$$

To estimate $\mathbb{E}[S_{x_0+\tau,\tau}(u)|\kappa_\tau]$, $u = 1, \ldots, T - \tau$, the first-order probit-Taylor approximation around an anchor scenario $\widetilde{\kappa}_\tau$ is given by

$$\Phi^{-1}\left(\mathbb{E}\left[S_{x_0+\tau,\tau}(u)|\kappa_\tau\right]\right) \approx D_{x_0+\tau,\tau}(u) + D'_{x_0+\tau,\tau}(u)(\kappa_\tau - \widetilde{\kappa}_\tau),$$

where $D_{x_0+\tau,\tau}(u) := \Phi^{-1}\left(\mathbb{E}\left[S_{x_0+\tau,\tau}(u)|\widetilde{\kappa}_\tau\right]\right)$ and

$$D'_{x_0+\tau,\tau}(u) = \frac{d}{d\kappa_\tau} \Phi^{-1} \left(\mathbb{E} \left[S_{x_0+\tau,\tau}(u)|\kappa_\tau \right] \right) \Big|_{\kappa_\tau = \widetilde{\kappa}_\tau}$$

$$= \frac{1}{\phi \left(\Phi^{-1} \left(\mathbb{E} \left[S_{x_0+\tau,\tau}(u)|\widetilde{\kappa}_\tau \right] \right) \right)} \left(\frac{d}{d\kappa_\tau} \mathbb{E} \left[S_{x_0+\tau,\tau}(u)|\kappa_\tau \right] \Big|_{\kappa_\tau = \widetilde{\kappa}_\tau} \right)$$

$$= \frac{1}{\phi \left(\Phi^{-1} \left(\mathbb{E} \left[S_{x_0+\tau,\tau}(u)|\widetilde{\kappa}_\tau \right] \right) \right)} \left(\mathbb{E} \left[\frac{d}{d\kappa_\tau} S_{x_0+\tau,\tau}(u) \Big| \widetilde{\kappa}_\tau \right] \right),$$

with

$$\frac{d}{d\kappa_\tau} S_{x_0+\tau,\tau}(u) = S_{x_0+\tau,\tau}(u) \cdot \left(-\sum_{s=1}^{u} \beta_{x_0+\tau+s-1} \cdot e^{\alpha_{x_0+\tau+s-1}+\beta_{x_0+\tau+s-1}\kappa_{\tau+s}} \right).$$

Finally, the expectations in $D_{x_0+\tau,\tau}(u)$ and $D'_{x_0+\tau,\tau}(u)$ need to be computed by simulation.

References

Avramidis, A.N., Hyden, P., 1999. Efficiency improvements for pricing American options with a stochastic mesh. In: Proceedings of 1999 Winter Simulation Conference. WSC, vol. 1. ACM, pp. 344–350.

Avramidis, A.N., Matzinger, H., 2004. Convergence of the stochastic mesh estimator for pricing Bermudan options. Journal of Computational Finance 7 (4), 73–91.

Broadie, M., Du, Y., Moallemi, C.C., 2011. Efficient risk estimation via nested sequential simulation. Management Science 57 (6), 1172–1194.

Broadie, M., Du, Y., Moallemi, C.C., 2015. Risk estimation via regression. Operations Research 63 (5), 1077–1097.

Broadie, M., Glasserman, P., 2004. A stochastic mesh method for pricing high-dimensional American options. Journal of Computational Finance 7 (4), 35–72.

Broadie, M., Glasserman, P., Ha, Z., 2000. Pricing American options by simulation using a stochastic mesh with optimized weights. In: Probabilistic Constrained Optimization. Springer, pp. 26–44.

Brouhns, N., Denuit, M., Van Keilegom, I., 2005. Bootstrapping the Poisson log-bilinear model for mortality forecasting. Scandinavian Actuarial Journal 2005 (3), 212–224.

Brouhns, N., Denuit, M., Vermunt, J.K., 2002a. A Poisson log-bilinear regression approach to the construction of projected lifetables. Insurance. Mathematics & Economics 31 (3), 373–393.

Brouhns, N., Denuit, M., Vermunt, J.K., et al., 2002b. Measuring the longevity risk in mortality projections. Bulletin of the Swiss Association of Actuaries 2 (1), 105–130.

Cairns, A.J., 2011. Modelling and management of longevity risk: approximations to survivor functions and dynamic hedging. Insurance. Mathematics & Economics 49 (3), 438–453.

Cairns, A.J., Blake, D., Dowd, K., Coughlan, G.D., Epstein, D., Ong, A., Balevich, I., 2009. A quantitative comparison of stochastic mortality models using data from England and Wales and the United States. North American Actuarial Journal 13 (1), 1–35.

Cairns, A.J., El Boukfaoui, G., 2021. Basis risk in index-based longevity hedges: a guide for longevity hedgers. North American Actuarial Journal 25 (sup1), S97–S118.

Chen, H., 2013. A family of mortality jump models applied to US data. Asia-Pacific Journal of Risk and Insurance 8 (1), 105–121.

Chen, H., Cox, S.H., 2009. Modeling mortality with jumps: applications to mortality securitization. The Journal of Risk and Insurance 76 (3), 727–751.

Czado, C., Delwarde, A., Denuit, M., 2005. Bayesian Poisson log-bilinear mortality projections. Insurance. Mathematics & Economics 36 (3), 260–284.

Dong, J., Feng, B.M., Nelson, B.L., 2018. Unbiased metamodeling via likelihood ratios. In: Proceedings of 2018 Winter Simulation Conference. WSC, pp. 1778–1789.

Dowd, K., Blake, D., Cairns, A.J., 2011. A computationally efficient algorithm for estimating the distribution of future annuity values under interest-rate and longevity risks. North American Actuarial Journal 15 (2), 237–247.

Dowd, K., Cairns, A.J., Blake, D., Coughlan, G.D., Epstein, D., Khalaf-Allah, M., 2010. Evaluating the goodness of fit of stochastic mortality models. Insurance. Mathematics & Economics 47 (3), 255–265.

Elvira, V., Martino, L., Luengo, D., Bugallo, M.F., 2019. Generalized multiple importance sampling. Statistical Science 34 (1), 129–155.

Feng, B.M., Staum, J., 2016. Green simulation designs for repeated experiments. In: Proceedings of 2016 Winter Simulation Conference. WSC, vol. 2016-Febru, pp. 403–413.

Feng, B.M., Staum, J., 2017. Green simulation: reusing the output of repeated experiments. ACM Transactions on Modeling and Computer Simulation 27 (4).

Fu, C., Fu, C., Michael, M., 2015. Handbook of Simulation Optimization. Springer Publishing Company, Inc.

Glasserman, P., 2004. Monte Carlo Methods in Financial Engineering, vol. 53. Springer.

Gordy, M.B., Juneja, S., 2010. Nested simulation in portfolio risk measurement. Management Science 56 (10), 1833–1848.

Hesterberg, T., 1988. Advances in importance sampling. Stanford University.

Hong, L.J., Juneja, S., Liu, G., 2017. Kernel smoothing for nested estimation with application to portfolio risk measurement. Operations Research 65 (3), 657–673.

Kim, J.H., Bae, T., Kim, S., 2017. Application of the phase-type mortality law to life contingencies and risk management. Applied Stochastic Models in Business and Industry 33 (2), 184–212.

Koissi, M.-C., Shapiro, A.F., Högnäs, G., 2006. Evaluating and extending the Lee-Carter model for mortality forecasting: bootstrap confidence interval. Insurance. Mathematics & Economics 38 (1), 1–20.

Lan, H., Nelson, B.L., Staum, J., 2010. A confidence interval procedure for expected shortfall risk measurement via two-level simulation. Operations Research 58 (5), 1481–1490.

Lee, R.D., Carter, L.R., 1992. Modeling and forecasting U.S. mortality. Journal of the American Statistical Association 87 (419), 659–671.

Li, J., 2014. A quantitative comparison of simulation strategies for mortality projection. Annals of Actuarial Science 8 (2), 281–297.

Li, J.S.-H., Li, J., Balasooriya, U., Zhou, K.Q., 2021. Constructing out-of-the-money longevity hedges using parametric mortality indexes. North American Actuarial Journal 25 (sup1), S341–S372.

Li, J.S.-H., Ng, A.C.-Y., 2011. Canonical valuation of mortality-linked securities. The Journal of Risk and Insurance 78 (4), 853–884.

Li, J.S.-H., Zhou, R., Liu, Y., Graziani, G., Hall, R.D., Haid, J., Peterson, A., Pinzur, L., 2020. Drivers of mortality dynamics: identifying age/period/cohort components of historical US mortality improvements. North American Actuarial Journal 24 (2), 228–250.

Lin, X.S., Liu, X., 2007. Markov aging process and phase-type law of mortality. North American Actuarial Journal 11 (4), 92–109.

Liu, M., Nelson, B.L., Staum, J., 2010. An efficient simulation procedure for point estimation of expected shortfall. In: Proceedings of 2010 Winter Simulation Conference. WSC. IEEE, pp. 2821–2831.

Liu, Y., Li, J.S.-H., 2015. The age pattern of transitory mortality jumps and its impact on the pricing of catastrophic mortality bonds. Insurance. Mathematics & Economics 64, 135–150.

Longstaff, F.A., Schwartz, E.S., 2001. Valuing American options by simulation: a simple least-squares approach. The Review of Financial Studies 14 (1), 113–147.

Mehdad, E., Kleijnen, J.P., 2018. Stochastic kriging for simulation metamodeling. Applied Stochastic Models in Business and Industry 34 (3), 322–337.

Owen, A.B., 2013. Monte Carlo theory, methods and examples. http://statweb.stanford.edu/~owen/mc/.

Renshaw, A.E., Haberman, S., 2008. On simulation-based approaches to risk measurement in mortality with specific reference to Poisson Lee-Carter modelling. Insurance. Mathematics & Economics 42 (2), 797–816.

Staum, J., 2009. Better simulation metamodeling: the why, what, and how of stochastic kriging. In: Proceedings of 2009 Winter Simulation Conference. WSC. IEEE, pp. 119–133.

Tsitsiklis, J.N., Van Roy, B., 2001. Regression methods for pricing complex American-style options. IEEE Transactions on Neural Networks 12 (4), 694–703.

Veach, E., Guibas, L.J., 1995. Optimally combining sampling techniques for Monte Carlo rendering. In: Proceedings of the ACM SIGGRAPH Conference on Computer Graphics. ACM, pp. 419–428.

Villegas, A.M., Millossovich, P., Kaishev, V.K., 2018. StMoMo: stochastic mortality modeling in R. Journal of Statistical Software 84 (3).

Yang, B., Li, J., Balasooriya, U., 2015. Using bootstrapping to incorporate model error for risk-neutral pricing of longevity risk. Insurance. Mathematics & Economics 62, 16–27.

Zhou, R., Li, J.S.-H., Tan, K.S., 2013. Pricing standardized mortality securitizations: a two-population model with transitory jump effects. The Journal of Risk and Insurance 80 (3), 733–774.